# Analyses of PDE-regulated phosphoproteomes reveal unique and specific cAMP signaling modules in T cells

Michael-Claude G. Beltejar

A dissertation

submitted in partial fulfillment of the

requirements for the degree of

Doctor of Philosophy

University of Washington

2017

Reading Committee:

Joseph Beavo, Chair

Shao-en Ong

Richard Gardner

Program Authorized to Offer Degree:

Molecular and Cellular Biology

University of Washington

## Abstract

Analyses of PDE-regulated phosphoproteomes reveal unique and specific cAMP signaling modules in T cells

Michael-Claude G. Beltejar

Chair of the Supervisory Committee:
Professor Joseph A. Beavo
Department of Pharmacology

Specific functions for different cyclic nucleotide phosphodiesterases (PDEs) have not yet been identified in most cell types. Conventional approaches to study PDE function typically rely on measurements of global cAMP, general increases in cAMP-dependent protein kinase (PKA), or exchange protein activated by cAMP (EPAC) activity. Although newer approaches utilizing subcellularly-targeted FRET reporter sensors have helped to define more compartmentalized

regulation of cAMP, PKA, and EPAC, they have limited ability to link this regulation to downstream effector molecules and biological functions. To address this problem, we used an unbiased, mass spectrometry based approach coupled with treatment using PDE isozyme-selective inhibitors to characterize the phosphoproteomes of the "functional pools" of cAMP/PKA/EPAC that are regulated by specific cAMP-PDEs (the PDE-regulated phosphoproteomes). In Jurkat cells we found multiple, distinct phosphoproteomes that differ in response to different PDE inhibitors. We also found that little phosphorylation occurs unless at least 2 different PDEs are concurrently inhibited in these cells. Moreover, bioinformatics analyses of these phosphoproteomes provides insight into the functional roles, mechanisms of action, and synergistic relationships among the different PDEs that coordinate cAMP-signaling cascades in these cells. The data strongly suggest that phosphorylation of many different substrates contribute to cAMP-dependent regulation of these cells. The findings further indicate that the approach of using selective, inhibitor-dependent phosphoproteome analysis can provide a generalized methodology for understanding the roles of different PDEs in the regulation of cyclic nucleotide signaling.

# TABLE OF CONTENTS

# LIST OF FIGURES

**Figure Number.**

# LIST OF TABLES

**Table Number**

# LIST OF ABBREVIATIONS

| | |
|---|---|
| AC | Adenylyl cyclase |
| ACN | Acetonitrile |
| CAM | chloroacteamide |
| cAMP | 3’,5’-cyclic adenosine monophosphate |
| cGMP | 3’,5’-cyclic guanosine monophosphate |
| EPAC | Guanine nucleotide exchange protein activated by cAMP |
| GEF | Guanine exchange factor |
| GO | Gene ontology |
| LC | Liquid chromatography |
| MS | Mass spectrometry |
| PDE | Phosphodiesterase |
| PFP | Predicted functional phosphosite |
| PKA | Protein kinase activated by cAMP |
| STRING | Search tool for the retrieval of interacting genes |
| TCEP | tris (2-carboxyethyl) phosphine |
| TFA | Trifluoroacetic acid |

# Acknowledgements

I wish to express my deepest gratitude to my advisor Professor Joseph Beavo. Your tremendous patience and support made this thesis possible. You have quite literally changed the trajectory of my life in more ways than one, and have assured that the renin/angiotensin signaling pathway will be forever engrained in my mind. There will never be enough thank you's for what you have done for me.

I would also like to thank the members of the Beavo lab. Thank you, Ira, for making sure I always received the necessary reagents, and for making sure I always had a seat on the 65. Thank you, Sergei for your support and council. Your enthusiasm for sharks in tornados reminds me to think outside the box… sometimes way outside the box. Thank you, Masami, for your kind words and encouragement. Science, like pounding mochi is arduous, but both usually end with satisfying results—thank you for helping me with both.

A special thanks to Dr. Thomas Hinds. I could not have weathered graduate school without your support. Thank you for all the professional and personal advice these many years. Mostly, thank you for constantly reminding me that growing old doesn't necessarily mean growing up.

A big thank you to Dr. Shao-en Ong and members of the Ong lab. Thank you for taking me into your lab and letting me use your mass spectrometry facilities. Thank you to Ho-Tak and Martin for reviewing the manuscript that comprises most of chapter 2.

To my brother, thank you for your unwavering support and giving me the pushes I needed at the times I needed them.

Thank you to my committee for your council and boundless patience.

Lastly, I would like to thank the University of Washington Molecular and Cellular Biology program, and the department of Pharmacology for the opportunity and means to pursue Ph.D. training.

# Dedication

For my sweethearts Maribel and Mochi

We did it!

# Chapter 1

# Introduction and Statement of Problem

The sheer density of proteins in a typical mammalian cell, 2-3 x $10^9$ proteins, in a volume of 2000-4000 $\mu m^3$ (Milo, 2013), necessitates a mechanism to reduce the frequency of nonspecific reactions, while retaining the ability to reliably execute numerous chemical reactions. Maintaining this balance is especially critical in the context of signal transduction wherein an aberrant (or absent) biochemical reaction, often among of series of reactions, could lead to the loss of signal fidelity, or premature termination. Eukaryotic cells have evolved over time to spatially and temporally organize chemical reactions into physical (organelles) and functional compartments (networks of scaffolds, protein complexes, and regions of biochemical activity) within the cell to promote an organized, and predictable response to stimuli. The pharmacological treatment and the concomitant perturbation of these functional compartments are essentially the basis of many investigative *in vitro* studies, as well as medicinal interventions for diseases such as cancer and inflammation. Therefore, to truly understand the impact of any given compound on a signaling cascade one needs to consider the constituents of these pathways, how they may be organized into functional compartments, and the molecular action of the compound on these constituents.

**Cyclic AMP is the prototypical second messenger**

In the late 1950's Earl Sutherland studied the hormonal action of epinephrine and glucagon on liver glycogenolysis. He observed two stages of hormone driven glycogen phosphorylase activation. First, epinephrine and glucagon stimulated the synthesis of a factor,

unaffected by heat inactivation, in the membranous pellet fraction of centrifuged liver homogenate. Second, this factor promoted the activation of glycogen phosphorylase, even in the presence of heat inactivated hormone. This indicated that it was in fact this unknown factor which drove phosphorylase activation (Berthet, Rall, & Sutherland, 1957). One year later, Sutherland identified the heat stable factor as 3',5'-cyclic adenosine monophosphate (cAMP), and suggested that a yet unidentified phosphodiesterase regulated its function(Rall & Sutherland, 1958). This seminal work spurred the discovery that many hormones signaled through cAMP to regulate a multitude of intracellular processes. Moreover, there were many other similar intermediary signaling molecules including: 3',5' cyclic guanosine monophosphate (cGMP), inositol trisphosphate, diacylglycerol, phosphatidylinositol, nitric oxide, carbon monoxide, and hydrogen sulfide. Collectively, the manner in which an extracellular stimulus is transduced into an intracellular signal, by an intermediary molecule became known as the second messenger signaling system.

The canonical cAMP signaling cascade begins when adenylyl cyclase (AC), the enzyme that catalyzes cAMP synthesis, is activated via ligand binding to a seven-transmembrane protein receptor. This causes a conformational change that results in an exchange of GTP for GDP on the Gα subunit in the Gα/Gβ/Gγ heterotrimeric guanine nucleotide exchange protein (G proteins). Upon Gα activation the G protein dissociates from the receptor and the α subunit dissociates from the βγ heterodimer. The signaling cascade bifurcates as Gα and Gβγ each bind to distinct downstream effector molecules. Based on amino acid sequences, Gα subunits are grouped into 4 subfamilies, Gβ subunits are grouped into two subfamilies, and Gγ subunits are grouped into 4 subfamilies(Downes & Gautam, 1999). Of particular relevance to cAMP signaling are members of the $G\alpha_s$ and $G\alpha_i$ subfamilies that respectively stimulate or inhibit

adenylyl cyclase. Signaling through Gβγ primarily inhibits the activity of adenylyl cyclase isoforms I, III, and VIII. However, Gβγ can also enhance forskolin activation of adenylyl cyclase isoforms II, IV, V, VI and VII(Brand, Sadana, Malik, Smrcka, & Dessauer, 2015). Therefore, modulation of cAMP synthesis is influenced by the ACs isoforms expressed, the constituents of the G protein, and how the G protein interacts with the GPCR—the combination of different GPCR binding domains of the three subunits confers receptor binding selectivity (Oldham & Hamm, 2008).

**Effector molecules downstream of cAMP**

Mechanistically, cAMP coordinates cellular responses by activating cAMP-dependent protein kinases (PKAs)(Walsh, Perkins, & Krebs, 1968), guanine nucleotide exchange factors (EPACs)(de Rooij et al., 1998), and cyclic nucleotide gated ion channels(DiFrancesco & Tortora, 1991). PKA is a serine/threonine kinase that preferentially phosphorylates the amino acid recognition sequence: Arg/Lys-Arg/Lys-X-Ser/Thr(Kemp, Benjamini, & Krebs, 1976; Kemp, Graves, Benjamini, & Krebs, 1977). Inactive PKA is a heterotetramer composed of two regulatory subunits and two catalytic subunits (Erlichman, Rubin, & Rosen, 1973). The regulatory subunit of PKA was first identified in bovine adrenal glands, as a protein that bound to radiolabeled cAMP, and first characterized as a negative regulator of the catalytic subunit(Gill & Garren, 1969, 1971). Four molecules of cAMP need to bind to the holoenzyme to activate PKA. Once activated the catalytic subunit is free to dissociate and phosphorylate downstream substrates(Builder, Beavo, & Krebs, 1980).

The EPAC superfamily are guanine nucleotide exchange factors (GEFs), activated by cAMP, for the small GTPase RAP1. The family is composed of three members: EPAC1, EPAC2, and Repac(de Rooij et al., 1998; Ichiba, Hoshi, Eto, Tajima, & Kuraishi, 1999;

Kawasaki et al., 1998). EPAC1 was discovered in Chinese hamster ovary cells (CHO) cells, when de Rooj et al observed that forskolin-stimulated cells increased the activated GTP-bound RAP1(de Rooij et al., 1998). EPAC1 and EPAC2 have common structural domains. Both proteins have a Dishevelled Egl-10, Pleskstrin (DEP) domain; Ras-exchanger motif (REM), and a guanine exchange factor domain (GEF), and lastly a cAMP binding domain. EPAC 2 has an additional lower affinity cAMP binding domain, and a Ras-association (RA) domain(de Rooij et al., 2000; Y. Li et al., 2006). The RA domain targets EPAC:RAS-GTP to the plasma membrane, and is another example of subcellular localization, and a mechanism to compartmentalize cAMP signaling.

The first cyclic nucleotide gated ion channel was cGMP-regulated and found in retinal tissue(Fesenko, Kolesnikov, & Lyubarsky, 1985). The first cAMP gated ion channel was found in olfactory cilia(Nakamura & Gold, 1987). In mammals six genes encode the four A subunits, and two B subunits of these channels. This family of channels are non-selective, and are $Ca^{++}$ permeant. These channels do not desensitize, and are regulated by phosphorylation and calmodulin binding. Channel response occurs with as little as one molecule of cyclic nucleotide, but the biggest response occurs when four cyclic nucleotides bind to the receptor.(D. T. Liu, Tibbs, Paoletti, & Siegelbaum, 1998)

**Phosphodiesterase regulation of cAMP signaling**

Phosphodiesterases are enzymes, grouped into 11 super families, that catalyze the hydrolysis of cyclic nucleotides into 5'AMP or 5'GMP. Therefore, PDE activity regulates the amplitude, duration, and subcellular localization of cyclic nucleotide signaling. The 11 family members are further subdivided into groups based on substrate specificity, structure, and common regulatory elements. All members share contain a conserved C-terminal catalytic core,

of approximately 250 amino acids. The N-terminal region typically contains several regulatory domains such as GAF (cGMP binding) domains, calmodulin binding domains, membrane targeting regions, and a PAS domain. PDEs 4, 7, and 8 exclusively hydrolyze cAMP. PDEs 5, 6, and 9 exclusively hydrolyze cGMP. PDEs 2, 3, 10, and 11 will hydrolyze both cAMP and cGMP. All PDEs are homodimers, except PDEs 1 and 6 which are heterotetramers.

**Compartmentalized cAMP signaling**

Studies in cardiac tissue provided some of the first evidence that compartmentalized, or pools of cAMP, existed in cells. There appeared to be a discrepancy between the actions of prostaglandin and β-adrenergic receptors on cardiac muscle contractility. While stimulating both receptors with agonist could raise cAMP to comparable levels, only β-adrenergic receptor stimulation increased contractile force and phosphorylase activity(Hayes, Brunton, Brown, Reese, & Mayer, 1979; Keely, 1979). Later confirmed in isolated cardiomyocytes, it was postulated that there existed two pools of cAMP in cardiomyocytes, and that a pool of cAMP which activated membrane bound PKA was responsible for causing changes in contractility(Buxton & Brunton, 1983; Corbin, Sugden, Lincoln, & Keely, 1977). Further investigation revealed that cAMP microdomains are shaped by the spatial organization of the hormonal receptors, ACs, and cAMP effector molecules(Cooper & Crossthwaite, 2006; Jurevicius & Fischmeister, 1996). Furthermore, gradients of cAMP are created by the activity of PDEs(Baillie, 2009).

In these microdomains PKA and PDEs can be tethered by A Kinase Anchoring Proteins (AKAPs)(Dodge et al., 2001; Hirsch, Glantz, Li, You, & Rubin, 1992). More recently, the EPAC1 and EPAC2 have been shown to occupy distinct subcellular regions in cardiomyocytes,

and RANBP2 has been shown to sequester EPAC1 to the perinuclear space(Gloerich et al., 2011; Pereira et al., 2015). The loss of cAMP localization and the dysregulation of PKA or EPAC signaling has been associated with several diseases including heart disease, glomerulonephritis, and chronic obstructive pulmonary disease (COPD) (Abboud, 1993; Omori & Kotera, 2007; Poppinga, Munoz-Llancao, Gonzalez-Billault, & Schmidt, 2014).

**Statement of problem**

It has become increasingly clear that compartmentalization is instrumental for properly regulating cAMP signaling cascades. From a basic sciences standpoint, compartmentalization can be studied by pharmacologically or by genetically disrupting PKA and AKAP interactions (Gold et al., 2013; Vijayaraghavan, Goueli, Davey, & Carr, 1997). Pools of cAMP can be increased by receptor selective agonists and by inhibiting PDEs. These approaches are very appropriate for defining and studying spatially constrained cAMP compartments. Yet from a clinical perspective the majority of patients will receive a systemic administration of a PDE inhibitor which will increase multiple pools of cAMP in many collective functional compartments, under multiple agonist stimulation. The challenge is to characterize these functional compartments, identify the molecular players involved, and ascribe biological functions regulated by creating these functional compartments.

In order to measure changes in the phosphoproteome of cAMP compartments, we coupled mass spectrometry based phosphoproteomic analyses with various selective PDE inhibitor treatments to characterize the PDE-regulated phosphoproteome of CD3/CD28-stimulated Jurkat cells. We used predictive tools to identify potential upstream regulatory kinases, metabolic pathways, and biological processes that can be regulated by different PDEs. To our knowledge, our study is the first to compare the phosphoproteomes of different functional

compartments sub-served by combinations of individual PDE isozymes in a T cell model. We observed unique phosphoproteomes associated with specific combinations of PDEs. Our data allows for the prioritization of future experiments to further understand how these pathways are regulated by specific PDEs. In addition our results have substantial implications for the design and use of selective PDE inhibitors in clinical practice.

# Chapter 2

# Proteomic Analysis of PDE Inhibitor Augmented cAMP Compartments

**Summary**

Inhibitors of cAMP PDEs are useful tools to study PKA/EPAC-mediated signaling and selective inhibitors for each of the 11 PDE families have been developed(Bobin et al., 2016; Chan & Yan, 2011; Nthenge-Ngumbau & Mohanakumar, 2017). The classical pharmacological approach to study cAMP-regulated systems has been to increase global cAMP *in vitro* or *in vivo* by means of adenylyl cyclase activation and/or treatment with relatively non-selective PDE inhibitors. Consequently, information about the composition and function of specific subcellular cAMP-signaling compartments was masked. Here, we utilize sets of highly selective PDE inhibitors to perturb putative cAMP compartment(s) combined with unbiased, global mass spectrometry (MS)-based analysis to capture dynamic changes in the phosphoproteomes regulated by these PDEs. We treated Jurkat cells with combinations of selective inhibitors to PDEs 1, 3, 4, 7, and 8, in the presence or absence of low, physiological concentrations of $PGE_2$. Total phosphorylation changes were quantified by label-free LC-MS/MS(de Graaf, Giansanti, Altelaar, & Heck, 2014; Jersie-Christensen, Sultan, & Olsen, 2016; Soderblom, Philipp, Thompson, Caron, & Moseley, 2011) leading to the identification of 13,589 sites, of which 618 were PDE inhibition sensitive. In doing so, we identify for the first time two distinct functional compartments regulated by two different combinations of PDE inhibitors.

Predictive algorithms were used to identify upstream regulatory kinases, and prioritize potential regulatory phosphosites for future investigation. The big advantage of this approach lies in the

unbiased identification of regulated phosphosites, and the sheer number of sites identified. To our knowledge, this is the first study to compare the phosphoproteomes of two functional compartments sub-served by any individual PDE isozyme or of any combinations of PDEs in a T cell model, not only in the basal state, but in an adenylyl cyclase stimulated state as well. We observed at least two functional pools of cAMP in Jurkat cells that are distinct from one another. The data underscore the need to understand the exact pharmacological response to individual and combinations of PDE inhibitors.

**Introduction**

Cellular signaling is a complex orchestration of multiple effector molecules making up communication relays that ultimately coordinate cellular responses. Since its original discovery nearly 60 years ago(Rall & Sutherland, 1958; Sutherland & Rall, 1958), cyclic 3',5' adenosine monophosphate (cAMP) has been shown to regulate numerous biological processes, in multiple cell types(Robison, Butcher, & Sutherland, 1968). Cyclic AMP coordinates cellular responses by activating cAMP-dependent protein kinases (PKAs)(Walsh et al., 1968), specific guanine nucleotide exchange factors (EPACs)(de Rooij et al., 1998), and cyclic nucleotide gated ion channels(DiFrancesco & Tortora, 1991). It also can directly regulate some of the cyclic nucleotide phosphodiesterases (PDEs). The PDEs comprise a family of enzymes that catalyze the hydrolysis of cAMP or cGMP to 5'-AMP or 5'-GMP, and thus regulate the amplitude, duration, and subcellular localization of cyclic nucleotide signaling.

It is thought that the expression and subcellular distribution of cAMP, PDEs(Chini, Grande, Chini, & Dousa, 1997), adenylyl cyclases(Cooper, 2005), effector molecules(Hasler, Moore, & Kammer, 1992), and target substrates are organized in such a way as to form "functional compartments". These compartments may correspond to known subcellular(Corbin

et al., 1977) regions or even be more diffuse and smaller than can be resolved by the light microscope. For example, PDE3B is localized predominately at membrane surfaces and is thought to regulate cAMP in regions proximal to these surfaces(H. Liu & Maurice, 1998). Similarly, in activated T cells, PDE4 is recruited to the T cell receptor, in a beta arrestin dependent manner, thus lowering cAMP in the vicinity of this part of the T cell activation pathway(Abrahamsen et al., 2004).

In T lymphocytes, PDE inhibitors and other agents that increase cAMP have been shown to reduce cell proliferation and bias T helper polarization towards $Th_2$, Treg, or $Th_{17}$ phenotypes(Boniface et al., 2009; Yao et al., 2009). Increased cAMP may even potentiate the T cell activation signal(Conche, Boulla, Trautmann, & Randriamampita, 2009), particularly at early stages of activation. Recent MS based proteomic studies have been useful in characterizing changes in the phosphoproteome of T cells under various stimuli such as: T cell receptor stimulation(Nguyen et al., 2016), prostaglandin signaling(Giansanti, Stokes, Silva, Scholten, & Heck, 2013), and oxidative stress(Ghesquiere et al., 2011).

## Materials and Methods

### Cell culture

Jurkat cell stocks (ATCC) ($5x10^6$) were thawed from frozen LN2 storage. Cells were cultured at 37ºC, 5% $CO_2$ for one week in RPMI, 10% FBS, 2mM Glutamine,100 U/ml Penicillin, and 100 µg/ml Streptomycin. 24 hours prior to experiment cells were washed and serum starved for 16 hours by culturing in RPMI in bacterial plates to prevent adhesion. After 16 hours, cells were synchronized by culturing in 50% FBS for two hours, washed twice with RPMI, followed by a 6-hour culture in serum free RPMI. To start the experiment, cells were

concurrently treated with the following reagents as described in the figures: 0.5 µg/ml CD3, 0.5 µg/ml CD28 (Miltenyi #s 130-093-387, 130-093-375), 1 nM prostaglandin $E_2$ (Cayman Chemical #14010), 200 nM IC0078 (PDE1i)(Intracellular Therapeutics), 5 µl cilostamide (PDE3i)(Tocris #0915), 10 µl rolipram (PDE4i)(Tocris #1349), 30uM BRL50481(PDE7i) (Tocris #2237), 200 nM PF-04957325 (PDE8i) (Pfizer), 50 µl IBMX (non-selective PDE inhibitor for all cAMP-PDEs except PDE8) (Sigma), or 200 µl IBMX. Treated cultures were incubated in 2 ml of media, in 2 ml microfuge tubes, at 37ºC, 5% $CO_2$ for 20 minutes.

**cAMP measurements**

Jurkat cells ($1X10^7$) were treated as previously stated. Cells were briefly centrifuged and the supernate discarded. Cell pellets were snap frozen in LN2, and stored at -80°C until analysis. Cell pellets were lysed by adding 1ml of 1:99 mixture of 11.65 M HCL: 95% EtOH. Pellets were dispersed using a P1000 pipet tip, and vortexed. Lysate was incubated at room temperature for 30 min. Following incubation, the extraction volume was transferred to a fresh microfuge tube, and dried in a speed vac. The cAMP was re-suspended in 150 µl of 0.1 M HCl, acetylated, and assayed using a cAMP ELISA kit according to manufacturer's recommendations (Cayman Biochemical).

**Immunoblot analysis**

Jurkat cells ($1X10^7$) were treated with PDE inhibitors as previously stated. Cells were briefly centrifuged and the supernate discarded. Cell pellets were snap frozen in LN2, and stored at -80C until analysis. Cells were lysed with 200 µl of Laemmli SDS buffer, vortexed briefly, and immediately placed in a boiling water bath. Samples were incubated for 7 minutes, vortexed, and centrifuged briefly. 20 µl was loaded onto 6 or 10% 1.5 mm poly-acrylamide Tris

Glycine SDS gels. Electrophoresis was run at 150 mV for 1 hour. Proteins were transferred to nitrocellulose at 34 mV for 16 hours. Immunoreactive bands were visualized and quantified using an Odyssey CLx imaging system using the 600 nm and 800 nm laser intensities set at 4 and 6 respectively. Membranes were blocked with PBS based Odyssey blocking buffer and then probed with primary antibodies in ½ diluted Odyssey blocking buffer containing 0.1% Tween20. Secondary antibodies 1:25,000 in ½ diluted Odyssey blocking buffer, containing 0.1% Tween20, and 0.05 % SDS. All incubations were 1 hour. Membranes were washed with PBS, 0.1% Tween20, for 5 minutes each wash, for a total of 3 washes. A final wash before visualization was in PBS. Image studio light v5.2 was used to quantify scans, and Graphpad Prism was used to graph results.

**Mass Spectrometry sample preparation**

Each biological condition was repeated a minimum of 3 times and a total of 3 analytical replicates each (minimum of 9 LC-MS/MS runs per condition) (Refer to Supplemental Figure 2 for experimental summary, and supplemental materials for details). A label-free mass spectrometry approach was used for these studies(Jersie-Christensen et al., 2016). After a 20-minute incubation with the indicated PDE inhibitors, adenylyl cyclase agonist, and CD3/CD28 antibodies, cells were centrifuged for 30 seconds at 20K x g. The supernate was aspirated and 250 µl of boiling lysis buffer added: 6M guanidinium hydrochloride, 100 µl Tris-HCl pH 8, 5 mM tris (2-carboxyethyl) phosphine (TCEP), and 10 mM chloroacteamide (CAM). Tubes were vortexed briefly, and placed in a boiling water bath for 10 minutes. Tubes were again vortexed briefly, and then centrifuged at 20K x g for 30 seconds. 3 µl of lysate was used for BCA protein quantification using a BSA standard, according to manufacturer's specifications (Pierce). One mg of lysate protein was transferred to a 1.5 ml, low binding microfuge tube (Axygen, MCT-

200-L-C). An equal volume of 25 mM Tris pH 8.0 and 1:200 Lys-C (wt/wt) was added. Lysates were incubated at 37°C, with 200 rpm shaking for 2 hours. After 2 hours, 1 ml of 25 mM Tris pH 8.0, and 1:100 (wt/wt) of 1mg/ml Trypsin (in 50 mM acetic acid) was added. Lysates were incubated overnight, for a minimum of 16 hours, at 37°C with 200 rpm shaking. Digests were then acidified with 1% Trifluroacetic acid (TFA), and centrifuged at 20K x g for 5 minutes. Supernates were applied to Waters Oasis 10mg extraction cartridges that were activated with reagents in the following order: 1 ml MeOH; 1 ml 80% Acetonitrile (ACN), 0.1% trifluroacetic acid (TFA); then 1 ml 5% ACN, 0.1% TFA. Supernates were passed through the cartridges via vacuum, and syringe plunger to prevent resin from drying. Cartridges were washed three times with 1 ml 5% ACN, 0.1% TFA. Peptides were eluted from cartridges with 500 µl 80% ACN, 0.1% TFA into a 1.7 ml low binding microfuge tube. Elution was repeated for a total of three times, and then the eluates combined and dried in a speed vacuum, at ambient temperatures.

For enrichment of phosphopeptides, dried peptides were re-suspended in 300 µl of 80% ACN, 0.1% TFA. Reconstituted peptides were transferred to 1.5 ml low binding microfuge tube with 20 µl of IMAC slurry, a 1:1:1 slurry of Fe-NTA, Ga-NTA, and PHO-Select Fe-NTA (Sigma). Peptides were incubated at 25°C for 1 hour with 1500 rpm shaking. Post incubation, tubes were centrifuged briefly, and the IMAC resin was washed with 500 µl of 80% ACN, 0.1% TFA. Washes were repeated for a total of two washes. IMAC resin was applied to C18 StageTips(Rappsilber, Ishihama, & Mann, 2003) (two punches of C18 membrane, Empore C18 #2315) and the volume was passed through with a syringe. The C18 was washed twice with 150 µl, of 1% formic acid. Phosphopeptides were eluted twice from the IMAC resin with 150 µl of 500 mM $K_2PO_4$. C18 resin was washed twice with 150 µl of 1% formic acid. StageTips were stored at 4°C.

**LC-MS/MS and data analysis**

Peptides were eluted from StageTips with 50 µl of 80% ACN, 0.1% TFA, into a 96 well, conical bottom, polypropylene plate. Phosphopeptides were dried in a speed vacuum and resuspended in 12 µl of 5% ACN, 0.1% TFA. 3 µl of phosophopeptides were applied to a self-pulled 360 µm OD x 100 µm ID 20 cm column with a 7 µm tip packed with 3 µm Reprosil C18 resin (Dr. Maisch GmbH, Germany). Peptides were analyzed in a 120 min, 5% to 30% acetonitrile gradient in 0.1% acetic acid at 300 nL/min on a nanoLC-MS (Thermo Dionex RSLCnano) and injected into an Orbitrap Elite. Orbitrap FTMS spectra (R = 30 000 at 400 m/z; m/z 350–1600; 3e6 target; max 500 ms ion injection time) and Top15 data dependent CID MS/MS spectra (1e4 target; max 100 ms injection time) were collected with dynamic exclusion for 30 s and an exclusion list size of 50. The normalized collision energy applied for CID was 35% for 10 ms. Mass spectra were searched against the Uniprot human reference proteome downloaded on July 29, 2015 and quantified using MaxQuant v1.5.2.8(Cox & Mann, 2008). Under group-specific parameters, all default parameters were retained. Under global parameters, match between runs were selected: match time window and alignment time window were set to 0.7 and 20 respectively. Data analysis was performed using the Perseus(Tyanova et al., 2016) suite.

**Kinase Prediction**

NetPhorest proposes kinases likely to phosphorylate queried sequences, based on the substrate consensus sequence motifs of 179 kinases. A trunctated peptide sequence of 4 amino acid residues flanking the regulated phosphosite was used as an input sequence in NetPhorest(Horn et al., 2014). The predictive threshold was set at 0.21.

**Functional Prediction**

The Predict Functional Phosphosites (pfp) database evaluates whether a phosphorylation at a specified amino acid is likely to alter protein function by evaluating the evolutionary conservation, degree of disorder, presence of structural features, and kinase association of the amino acid sequence containing the modification site. The same trunctated peptide sequence of 4 amino acid residues flanking the regulated phosphosite was used as an input sequence to query the database: pfp_database_release_1_2_update_1__20160126. Downloaded from http://pfp.biosino.org/pfp/(Xiao, Miao, Bi, Wang, & Li, 2016)

**STRING (Search Tool for the Retrieval of INteracting Genes) analysis**

For each series of PDE inhibitor treatments, all statistically significant regulated phosphosites were compiled and lists of unique proteins were generated. Each protein list was used to query the STRING interaction database(Szklarczyk et al., 2015) (http://string-db.org/). "Experiments" and "Databases" source options were selected, and the minimum interaction score was set to 0.700. For visual clarity, disconnected nodes were omitted from the interaction map.

**Gene ontology analysis**

Gene ontology (GO) analysis was performed using the ClueGo Cytoscape plug in(Bindea et al., 2009). Lists of unique proteins, for each series of PDE inhibitor treatments, were generated from the statistically significant regulated phosphosites. Each list was used to query Kegg, Gene Ontology—biological function database, and Wikipathways. ClueGo parameters were set as indicated: Go Term Fusion selected; only display pathways with p values $\leq 0.05$; GO tree interval, all levels; GO term minimum # genes, 3; threshold of 4% of genes per pathway; and a kappa score of 0.42. Gene ontology terms are presented as nodes and clustered together

based on the similarity of genes present in each term or pathway. Node size is proportional to the P value for GO term enrichment, i.e. a larger node is generated from a smaller P value. Proteins are presented as smaller circles. Multicolored circles indicate proteins associated with more than one process.

## Results

### Global cAMP levels are elevated only by specific combinations of PDE inhibitors.

To determine which sets of PDE inhibitors to use in phosphoproteomic studies, we first treated Jurkat cultures with individual isozyme-selective PDE inhibitors or various combinations of inhibitors, and then measured the resulting changes in cAMP levels. Previous studies, as well as our own qPCR data (not shown), identified PDEs 1B, 1C, 3B, 4A, 7A, 8A, and 9A mRNA as being most highly expressed in Jurkat cells(Bloom & Beavo, 1996; Dong, Zitt, Auriga, Hatzelmann, & Epstein, 2010; Erdogan & Houslay, 1997). In theory, any of these PDEs or combination of PDEs could regulate different functional cAMP compartments in the cell. We also used 50 μM and 200 μM IBMX (a potent, general, non-selective inhibitor) and 200 nM PF-04957325 (a PDE 8 selective inhibitor) to inhibit the majority of cAMP hydrolyzing PDEs. We then chose those inhibitor combinations that seemed most likely to influence the greatest number of PDE-regulated functional compartments for follow-up by phosphoproteomic analysis (Figure 1; Supplemental Figure 1).

Unexpectedly, the individual PDE inhibitor treatments alone did not cause a significant increase in total cAMP either in the absence (data not shown) or the presence of low $PGE_2$ (1nM) (Figure 1). However, when combined with a low concentration of $PGE_2$ (1 nM), the combination of cilostamide (PDE3i) and rolipram (PDE4i) treatment greatly increased cAMP, from 9.7 pmol/ml to 144 pmol/ml (Figure 1). Interestingly, the combination of $PGE_2$ plus 50 μM IBMX

and 200 nM PF-04957325 (PDE8i) increased cAMP to a lesser degree (9.7 pmol/ml to ~50 pmol/ml) compared to $PGE_2$ plus cilostamide and rolipram, perhaps due to the known antagonistic effect of IBMX on adenosine stimulated cAMP. However, a higher concentration of IBMX (200 μM) and 200 nM PF-04957325, plus $PGE_2$ (1nM) increased cAMP approximately 30-fold (6.6 pmol/ml to 200 pm/ml) (Supplemental Figure 1). In these conditions, the highest level of cAMP was seen in the presence of a supersaturating concentration of 200 μM $PGE_2$ (Figure 1). Overall, the results indicated that most putative cAMP compartments would not be saturated except perhaps in the high $PGE_2$ condition, therefore implying that it could be feasible to use lower PDE inhibitor combinations to begin to resolve the PDE-specific functional compartments in the cell.

**Phosphoproteomic interrogation of PDE functional compartments (the PDE-regulated phophoproteomes).**

To identity the constituents of putative PDE-regulated compartments, we designed a phosphoproteomic approach utilizing the combination of PDE inhibitors which caused the greatest increases in global cAMP based to our cAMP assay results. This approach is illustrated in Supplemental Figure 2A. Preliminary analysis of the number of phosphopeptide identifications in the basal condition, Supplemental Figure 2B, suggested that near maximal identification, for our instrumentation and sample preparation, could be achieved with a minimum of 9 LC-MS/MS runs for each treatment condition (≥ 3 biological replicates and 3 analytical replicates each). A single LC-MS/MS run yielded on average 5146 unique phosphophopeptides quantified and increasing the number of LC-MS/MS runs to 9, approached a plateau number of phosphopeptides to ~10,000 per biological condition (Supplemental Figure 2B). The Pearson correlation coefficients between biological replicates and analytical replicates

were between 0.5 – 0.9 and ≥ 0.9, respectively (Supplemental Figure 2C). In total, we identified 13,589 phosphopeptides and 3241 proteins. For further downstream functional analyses, we only included phosphopeptides that were observed in at least 60% of the LC-MS/MS runs in the respective treatment groups. Of the 13,589 phosphopeptides identified, we found 618 phosphopeptides distributed among 461 unique proteins were significantly regulated by the PDE inhibitor treatments (False discovery rate ≤ 0.05, two-tailed t-test, permutation-based FDR. (Please refer to supplemental_materials.xls for the complete list).

**Different PDEs regulate distinct functional compartments.**

Consistent with the cAMP assays, no phosphosites were significantly altered by individual PDE inhibitor treatments alone under the basal condition (no $PGE_2$) (data not shown) or in the 1 nM $PGE_2$ stimulated state (Figure 2A). However, we observed a synergistic increase in phosphopeptides identified when two or more PDEs were inhibited (Figure 2A, Supplemental Figure 4). To corroborate the proteomics data, we used a commercially available antibody (Abcam) to probe for changes in Stathmin1 S63 phosphorylation (a phosphosite identified in our proteomics study) in response to PDE3 and 4 inhibition. In agreement with the proteomics study, we found that neither PDE3 nor PDE4 inhibitors alone caused a change in phosphorylation. However, inhibition of both PDEs increased S63 phosphorylation. In this case, treatment with 200 μM IBMX plus the PDE8 inhibitor caused the greatest increase in phosphorylation (Figure 2B).

We also attempted to define functional compartments regulated by other PDEs, and not just PDEs 3 and 4. So, we performed the same analysis with 50 μM IBMX plus 200 nM PF-04957325 and 200 μM IBMX plus PF-04957325. We expected that the 200 μM IBMX plus PF-04957325 condition would likely define the total “PDE-regulated functional compartments”. We

assessed each of these conditions in the absence or presence of a low concentration $PGE_2$ (1 nM). Indeed, many more regulated-phosphosites were modulated when all PDEs were inhibited (Figure 3). We surmised that the remaining PDEs (i.e. not PDEs 3 and 4) which included PDEs 1, 7, and 8 (or some combination thereof) might also sub-serve different, non-overlapping functional compartments from those regulated by PDE 3 and/or PDE4. Therefore, we also treated Jurkat cells with a combination of IC0078 (PDE1i), BRL50481 (PDE7i), and PF-04957325 (PDE8i), in the absence or presence of $PGE_2$ (1 nM).

The subset of cilostamide and rolipram regulated phosphosites made up a portion of the total IBMX and PF-04957325-regulated phosphosites (Figure 3, left panel). Forty phosphosites were selectively regulated by inhibiting PDEs 3 and 4, and not by inhibiting PDEs 1, 7, and 8 (Figure 3, Table 1). Table 2 shows examples of phosphosites increased by the combination of PDEs 3 and 4 inhibitors in the absence and presence of $PGE_2$ (for the full list, refer to supplemental_materials.xls). Under $PGE_2$ stimulated conditions, 66 and 123 phosphosites were regulated by PDEs 3 and 4, and PDEs 1, 7, and 8 treatment groups, respectively (Figure 3, right panel). Yet, even with increased peptide identification, only one common phosphosite was regulated by both PDE inhibitor treatment groups - Slingshot Protein Phosphatase 2, SSH2 (S811). This general non-overlap strongly suggested that the functional pool(s) of cAMP regulated by the combination of PDEs 1, 7, and 8 inhibitors are different than the pool(s) regulated by the combination of PDEs 3 and 4 inhibitors and that perhaps SSH2 is regulated by cAMP in more than one functional compartment (Figure 3, right panel and Table 2).

**Identifying kinases that regulate PDE-regulated phosphoproteomes.**

Distinct functional pools of PDE-regulated phosphosites were further characterized by identifying the regulatory kinases predicted to be the most likely responsible for phosphorylating

the queried sites. Analysis of the sequences of the phosphosites with the program, NetPhorest(Bozza, Payne, Goulet, & Weller, 1996), a web based tool for kinase prediction (*https://omictools.com/**netphorest**-tool*), suggested that the majority of phosphosites regulated by inhibition of PDEs 1,7, and 8 are primarily phosphorylated by casein kinase II or a kinase with a similar substrate recognition motif, both in the basal and $PGE_2$ stimulated conditions (Figure 4, left panels). By contrast, the same algorithm suggested that most of the phosphosites increased when inhibiting both PDEs 3 and 4 are primarily phosphorylated by PKA (Figure 4, right panels). We observed a similar trend in $PGE_2$ stimulated cells. The majority of sites predicted to be phosphorylated by PKA contain a modified S/T residue contained in the classic PKA consensus motif R/L, R/L, X, S/T—red bars (Supplemental Figure 3B and 3D). However, 132 of 151 phosphorylation sites in the PDE 1, 7, and 8 inhibitor-treated cells did not contain this predicted PKA consensus site (Supplemental Figure 3A and 3C).

**Prioritizing phosphosites with likely biologically relevance**

To identify possible, biologically relevant phosphosites, we searched a database of proteins with phosphosites annotated for predicted regulatory function(Xiao et al., 2016). This database was compiled by Xiao et al. using an algorithm that compared the sequence of the phosphosite with a series of criteria including: evolutionary conservation, secondary structure, regional disorder, and the degree of sequence similarity to kinase recognition motifs between known functional and background phosphorylation datasets. Of the 618 sites that were significantly modulated by PDE inhibitor treatment, 160 were predicted by this algorithm to be "likely" to have a regulatory function (refer to supplemental_materials.xls for the full list). In fact, 55 of these identified phosphosites had annotations in the PhosphositePlus(Hornbeck et al.,

2015) database, indicating that there was empirical evidence demonstrating that phosphorylation at the identified sites regulated protein function (examples in Table 3).

We identified a series of phosphosites for which a regulatory role had not yet been empirically determined. Several examples for PDEs 1, 7, and 8 are shown in Table 4 and for PDEs 3 and 4 are shown in Table 5. We found 50 potential regulatory sites in the PDEs 1, 7, and 8 inhibitor group (Table 4) and 30 potential regulatory sites in the PDE 3 and 4 inhibitor group (examples in Table 5). Clearly, these sites are prime candidates for further follow-up with genetic and mutagenesis approaches to corroborate possible new molecular functions for these PDE-modulated phosphosites.

**Interaction Networks defined by STRING analysis**

We used STRING analysis (Szklarczyk et al., 2015) as another method to suggest which biological processes or pathways might be regulated in each PDE inhibitor treatment group, and further prioritize which phosphosites warranted further investigation. Our STRING analysis identified proteins that have been empirically shown to interact ("experiment" option), or are known components of an annotated common pathway ("database" option). This analysis showed a greater number of interacting proteins in the PDE 1, 7, and 8 inhibitor treatment group compared to the PDE 3 and 4 inhibitor treatment group (Figure 5). As expected, the greatest number of interactions were observed in the 200 µl IBMX plus PDE 8 inhibitor treatment group (Supplemental Figure 5). Under default network visualization settings, in the PDE 1,7, and 8 condition, there are clusters of interacting proteins around MAPK3/ERK1, HDAC4, and POL2RA (Figure 5). The PDE3 and 4 combination shows a cluster of interacting proteins around RANBP2 (Figure 5). Lastly, when all PDEs were inhibited by IBMX plus PDE8i, clusters of proteins interacting with HDAC1, SIN3A, MAPRE1, ARHGEF7, ABL1, LCK,

CHEK1, and PRKAB1 are visible (Supplemental Figure 5). Each of these clusters are indicative of proteins associated with particular pathways or functions. The observation that cAMP is modulating several members of a cluster most likely suggests that cAMP regulates a process along multiple points of the pathway/process.

**Identification biological processes regulated by specific combinations of PDE inhibitors.**

In order to identify the processes that could be regulated by respective PDE inhibitor treatments, we used GO analysis (Gene Ontology analysis) of the list of phosphoproteins regulated by PDE 1, 7, and 8 inhibitor treatment grouped 90 of 133 genes into 17 functional clusters (Supplemental Figure 6 and Supplemental Table 1). Figure 7A shows an example of 6 identified functional clusters and the genes associated with their respective processes. GO analysis of the combination of PDE 3 and 4 inhibitor treatment sites resulted in 20 of 74 genes grouped into 6 functional clusters. (Figure 7B) and (Supplemental Table 2.) GO analysis of the 200 µM IBMX treatment data resulted in 317 of 368 genes grouped into 34 clusters. It is likely that these different combinations of PDE inhibitors sub-serve different functional pools of cAMP and that the different functional pools in turn regulate the different functions identified by the GO analysis. It should be noted that particularly in the presence of $PGE_2$, there are several common gene products identified in both the PDE 3 plus 4 inhibitor condition and the PDE 1, 7, and 8 inhibitor condition. However, in general the sites that are phosphorylated by the different PDE inhibitor combinations are different. Several possibilities for this observation are discussed in the next section.

**Discussion**

In this study, we used a non-biased mass spectrometry phosphoproteomics approach coupled with isozyme-selective PDE inhibitors to identify some of the PDE-regulated

phosphoproteomes modulated by several different cAMP-PDEs" in a model T cell line. According to Ponomarenko(Ponomarenko et al., 2016) there are over 20,000 different proteins in the human proteome, not including splice variants and post-translationally modified proteins. No single cell is expected to express all possible proteins at all times. In our studies, we identified 3241 phosphorylated proteins containing 13,589 phosphopeptides present in CD3/CD28 stimulated Jurkat T-cells. The number of phosphophopetides we identified were comparable to the number of phosphopeptides identified in other mass spectrometry studies, characterizing the Jurkat phosphoproteome, utilizing different MS paradigms: 10,500 by Mayya et al.(Mayya et al., 2009), 11,454 Salek et al(Salek et al., 2013), and 12,799 de Graaf et al(de Graaf et al., 2014). Of these 13,589 phosphopeptides, 618 were significantly regulated by specific combinations of selective PDE antagonists compared to DMSO, or $PGE_2$ controls. Nine LC-MS/MS runs were sufficient to identify ~88% of the enriched phosphopeptides per biological condition. We observed very high correlation between analytical LC-MS/MS replicates with > 0.9 Pearson correlation coefficient. There was greater variation between biological replicates that we attribute to inherent variations in culture conditions and sample processing.

We defined the "PDE-regulated functional compartments" as those containing proteins that are acutely modulated by a selective PDE inhibitor treatment. Using the subset of conditions and drugs that we studied, we observed at least three distinct functional compartments regulated by PDEs: first, those regulated by a combination of PDEs 1, 7, and 8 inhibitors; second, those regulated by the combination of PDE 3 and 4 inhibitors; and third, those regulated by the combination of IBMX and a PDE8 inhibitor that were not regulated by the other two combinations. It is quite likely there will be additional functional compartments identified as different combinations of PDE inhibitors are investigated. Of note, it was necessary to inhibit

both PDE3 and PGE4 to elicit any changes in this compartment. Individual PDE inhibitors had little or no effect by themselves. However, neither PDE3 inhibitors nor PDE4 inhibitors were coupled with inhibitors of any of the other PDEs expressed in the Jurkat cells. As the combination of IBMX plus the PDE8 inhibitor yielded many more phosphosites than the combined total of the PDE3 and PDE4 inhibitors and the combination of PDE 1,7, and 8 inhibitors, it seems quite likely that other combinations of PDE inhibitors will give different and expanded PDE-regulated phosphoproteome signatures.

In general, the PDE inhibitor effects on the phosphoproteome correlated well with the observed changes in cAMP caused by the same PDE inhibitor treatments. This indicated that the concentrations of cilostamide (5uM) and rolipram (10uM) used, even though predicted to elicit ~ 90% inhibition of PDE3s and PDE4s, respectively, were still selective as neither treatment alone could regulate either cAMP or the phosphoproteomics data. The non-selective inhibitor, IBMX (200 µl) plus PF-04957325 (200 nM) should in theory inhibit all cAMP-PDEs. This combination caused the greatest number of changes in regulated sites, both in the basal and $PGE_2$ stimulated states. As mentioned above, this also indicates that there are other functional compartments regulated by different combinations of PDEs that remain to be identified and annotated. Both the phosphoproteomic results and the changes in cAMP seen in response to the PDE inhibitor treatments also indicated that these compartments are most likely not regulated by single PDEs. It is possible that these remaining functional cAMP compartments may be sub-served by 3 or more PDEs. Unfortunately, we could not perform phosphoproteomic studies under all the possible combinations of PDEs 1, 7, and 8 inhibitors much less all combinations of all PDE inhibitors. We acknowledge these studies will need to be done to understand the full "PDE-regulated phosphoproteomes".

It is perhaps worth repeating that the largest cAMP and phosphorylation changes were seen in the $PGE_2$ stimulated conditions, both in the phosphoproteome and cAMP data compared to the basal condition. As a result, it appeared that these functional compartments were dynamic and could be influenced by the source of cAMP. Therefore, it is plausible that the functional compartment(s) defined by PDEs 1, 7, and 8 inhibition or the PDE 3 plus 4 conditions could be different in for example adenosine stimulated cells versus $PGE_2$ stimulated cells. Additionally, the time course studies by Giasanti et al(Giansanti et al., 2013), and Golkowski et al.(Golkowski, Shimizu-Albergine, Suh, Beavo, & Ong, 2016) would suggest that these functional compartments changed in time as well. The time frame for such phosphorylation changes may be different between PDE inhibitor treatements, suggesting an additional parameter that would need to be explored in order to fully understand the scope of the functional "PDE-regulated phosphoproteome". Clearly a more comprehensive study of cAMP/PDE functional compartments would be needed to investigate all the possible combinations of PDE inhibitors under multiple agonist stimulation paradigms.

**Direct phosphorylation by PKA.**

Of the 618 significantly regulated phosphosites, 55 are annotated in PhosphositePlus indicating that, when phosphorylated, these sites had been empirically determined to directly or indirectly regulate protein function. Of these, 14 phosphosites were at canonical PKA consensus sequences and therefore are likely to be directly phosphorylated by PKA. These include: ARFIP1- S132(Cruz-Garcia et al., 2013; Gehart et al., 2012), ARHGEF2- S886(Meiri et al., 2009), BAD- S152(Lizcano, Morrice, & Cohen, 2000; Zhou, Liu, Payne, Lutz, & Chittenden, 2000), BRAF- S446(Tran, Wu, & Frost, 2005), CAD- S1406(Kotsis et al., 2007), CAMKK1- S458(Wayman, Tokumitsu, & Soderling, 1997), KIF3A- S687(Phang et al., 2014; Xiong et al.,

2015), LASP1- S146(Butt et al., 2003; Mihlan et al., 2013; Vaman et al., 2015), PTPN7-S44(Nika et al., 2006; Saxena, Williams, Tasken, & Mustelin, 1999), RCC1- S11(Hood & Clarke, 2007; Horiike, Kobayashi, & Sekiguchi, 2009; Hutchins et al., 2004), RPS6-S235(Wettenhall & Morgan, 1984), STMN1- S63(Beretta, Dobransky, & Sobel, 1993; Marklund et al., 1994; Yip, Yeap, Bogoyevitch, & Ng, 2014), and TAL1- 172(Y. Li et al., 2012; Prasad & Brandt, 1997). In fact, eight of them including, ARHGEF2, BAD, CAD, CAMKK1, LASP1, PTPN7, STMN1, and TAL1 had been reported as substrates of PKA at the aforementioned sites in other cell types. This result also tended to corroborate the combined inhibitor-phosphoproteomic approach outlined in this manuscript. Moreover, these proteins are associated with a wide array of biological functions, and would indicate that cAMP coordinates not just a few rate-limiting steps but rather a large number of sites that in turn regulates multiple processes in the T cells. In fact, this observation may call into question the generally taught concept that only a single "rate limiting" step is likely to be the major regulatory site for cAMP/PKA in many pathways.

As alluded to above, these regulatory sites should not be interpreted as exclusively PKA substrates. STMN1 S63, RCC1 S11, and PTPN7 S44 can also be phosphorylated by CaMKIV(Marklund et al., 1994), CDK1(Hutchins et al., 2004), and PKCϴ(Saxena et al., 1999) respectively. It is plausible therefore and perhaps even likely that the sequences of these sites have evolved so that different kinases can regulate the same site under specific but differing cellular contexts. Nonetheless, the identification of these phosphosites also validated the mass spectrometry approach to identify biologically relevant phosphosites in response to combinations of PDE inhibitor treatments. This encouraged us to expand our analysis beyond sites with canonical PKA consensus sequences in order to identify other PDE-dependent phosphosites with

probable regulatory actions because they could lead to identification of novel molecular mechanisms by which cAMP and PDEs coordinate cellular responses.

**PDE synergies - Inhibition of multiple PDEs is needed to regulate individual sites and processes.**

The majority of phosphosites were not regulated until more than one PDE was inhibited. This may, in part, provide a molecular explanation for the observations of Giembycz and others that only when both PDEs 3 and 4 were inhibited did the proliferation of primary T cells decrease. (Giembycz, Corrigan, Seybold, Newton, & Barnes, 1996) That is, molecular effectors controlling proliferation are only well regulated by PDE inhibition when more than one PDE is inhibited.

The many examples of PDE synergy in the current datasets, at both the cAMP and PDE-regulated phosphoproteome level, could also have a substantial implication for drug design. Data from a clinical study by Franciosi et al.(Franciosi et al., 2013) showed that RPL554, a dual PDE 3 and PDE 4 inhibitor, was an effective bronchodilator, and reduced inflammation in patients with COPD. While perhaps not yet fully embraced by the pharmaceutical industry, an increasing number of such functional examples are being elucidated whereby multiple PDEs need to be inhibited in order to elicit a pharmacological response. To our knowledge, very few such screening studies have been done previously. The current data not only demonstrated this same PDE synergy principle at a molecular level, but indicated that a phosphoproteomic approach could be used as a part of an initial preclinical screen to determine which PDEs need to be inhibited to maximize a therapeutic effect or to minimize an unwanted side effect.

**PDE 1, 7, 8 - regulated functional compartment(s).**

Interestingly, the functional compartment(s) regulated by PDEs 1, 7, and 8 have differing characteristics compared to the compartment(s) regulated by PDEs 3 and 4. The stark differences between these two functional compartments were not fully expected. We found for example that the majority of sites regulated by PDEs 3 and 4 have a PKA consensus sequence, and NetPhorest analysis predicted that the majority of these sites would be phosphorylated by PKA. This strongly suggested that they are direct substrates of PKA and/or perhaps also other AGC type kinases. By contrast, much greater diversity of kinases is predicted to regulate the phosphosites in the PDE 1, 7, and 8 compartment(s). Moreover, the majority of sites regulated in these compartments do not have a PKA consensus sites. In both the basal and $PGE_2$ stimulated state, CK2 is the predominately predicted kinase for this functional compartment. One possible mechanism here is that cAMP could be activating PKA or EPAC upstream of CK2, and the effects of cAMP while real are indirect. If so, this represents a new unexplored mechanism of cAMP action. There also may be effects of PDEs 1, 7, and 8 inhibitors on phosphatase activity.

**Biological Processes Regulated by different PDE-regulated phosphoproteomes.**

Gene ontology analysis was performed to provide insight into what biological processes might be regulated by each series of PDE inhibitor combinations. We observed that the biological processes regulated by inhibition of PDEs 1, 7, and 8 were largely distinct from those regulated by inhibition of PDEs 3 and 4 as might be expected since the proteins phosphorylated are also different. While functional clusters such as spindle organization, regulation of cytoskeleton and double stranded break repair are common to both treatment groups, it is worth noting that the genes present in each node are different among treatment groups. This indicated that inhibition of different combinations of PDEs may affect the same biological process but via different mechanisms. A number of the biological processes identified by GO analysis have

been previously reported to be regulated by cAMP. These include mRNA splicing(Aksaas, Eikvar, Akusjarvi, Skalhegg, & Kvissel, 2011; Jarnaess et al., 2009; H. Li et al., 2009), spindle organization(Gharibi et al., 2013; Vandame et al., 2014), fibroblast migration(Olmedo et al., 2013; Sinha et al., 2015), lamellipodium assembly(Chen, Zhang, & Huang, 2008; Heasman & Ridley, 2010), apoptosis(Gupta et al., 1999; Ivanov, Lee, Podack, & Malek, 1997; Lalli, Sassone-Corsi, & Ceredig, 1996; Zhang et al., 2008), ATM signaling(Cho, Kim, Kwak, & Juhnn, 2014; Eliezer, Argaman, Kornowski, Roniger, & Goldberg, 2014), gene silencing via micro RNA(Feng, Yan, Li, & Hou, 2016; Huang et al., 2009; P. Li, Xue, Feng, & Mao, 2015; Vo et al., 2005), T cell selection(Vig et al., 2002), and cytoskeletal reorganization(Howe, 2004). However, this is one of the first studies to indicate molecular substrates that might participate in the regulation of these processes. To date the role(s) of cAMP/PKA signaling is even less well defined for most of the other biological processes implicated, such as chromatin remodeling(Clapier & Cairns, 2009; Hedrich et al., 2014; Lai & Wade, 2011) and chromosomal segregation. Again, the phosphopeptides that map to these processes should be a good place to start mechanistic studies of cAMP/PDE effects on these processes.

STRING analysis of the PDE 1,7, and 8 inhibitor phosphosites, suggests a cAMP mediated regulatory action on the phosphatase, PTPN7, a known regulator of MAPK3 and other kinases in this cascade. There are 15 phosphosites modulated under the PDE 1, 7, and 8 inhibitor condition that are predicted to be phosphorylated by MAPK3. Likely examples of indirect cAMP signaling via phosphatase regulation include: BAP18 S76, CHAMP1 S286, CHD3 S1660, CHD3 S1660, ITPKB S43, LIN9 S380, LMNB1 S391, NCOR1 S2048, PIK33C2A 1553, RB1 T778, RING1 S254, SMEK1 S728, SNIP1 S54, SNTB2 S393, AND STAT1 S727.

Interestingly, Conche et al.(Conche et al., 2009) previously implicated PTPN7, ERK, and a cAMP mediated signal as an early enhancer of the T cell receptor response promoted by cellular adhesion. We found that phosphosites on ARHGEF2, BRAF, LASP1 and PTPN7 were regulated by inhibiting PDEs 1, 7, and 8; whereas sites on CAD, BAD, CAMKK1, PTPN7, and STMN1 were regulated by inhibiting PDEs 3 and 4. ARHGEF2(Meiri et al., 2012), BRAF(Brown, Khalili, Rodriguez-Cruz, Lizee, & McIntyre, 2014), and LASP1(Mihlan et al., 2013) have been associated with regulation of cytoskeletal organization and cell adhesion/migration. It is plausible that inhibiting a combination of PDEs 1, 7, and 8 could therefore regulate T cell migration and activation. Since PDE1 protein and activity is reported to be low in several T cell models, this perhaps suggests that the most important combination will be PDE7 and PDE8 inhibitors.

PDE 3 and 4 inhibition also significantly increased the phosphorylation of CAD (Table 2), the rate limiting protein in the pyrimidine biosynthetic pathway. Increased glutamine metabolism in lymphocytes is thought to be required to support proliferation, and provide metabolites for biosynthetic pathways(Nakaya et al., 2014; Newsholme, Crabtree, & Ardawi, 1985; Sugimoto et al., 2015). CAD is a multi-domain protein that catalyzes the first reactions of de novo pyrimidine biosynthesis, converting glutamine to carbamoyl phosphate. UTP binding to the BH3 regulatory domain of CAD, causes feedback inhibition. Phosphorylation of S1406 prevents UTP binding and increases activity of the enzyme(Kotsis et al., 2007). Paradoxically, it seems that phosphorylation of S1406 on CAD would increase glutamine metabolism and promote T cell activation. However, the combination treatment of PDEs 3 and 4 inhibitor has been shown to inhibit T cell function. One possible explanation is that an overactive pyrimidine biosynthetic pathway reduces the available glutamine that can be converted to glutamate and

shuttled into the TCA cycle or converted to glutathione. This should reduce the cells ability to buffer against reactive oxygen species generated by rapid proliferation, and could be a novel mechanism of cAMP-dependent inhibition of T cell function.

Similarly, S163 of DGKZ is one of the most consistently phosphorylated sites in the PDE3 plus PDE4 inhibitor condition. A number of T cell functions are known to be controlled by DGKZ(Krishna & Zhong, 2013). For example, it is well established that redistribution of diacylglycerol kinase to the immunological synapse can regulate several aspects of T cell activation(Gharbi et al., 2011) and function including T cell adhesion and migration(Baldanzi, Bettio, Malacarne, & Graziani, 2016). Activation of DGKZ would be expected to lower diacylglycerol and increase phosphatidic acid, both of which are likely to decrease T cell activation. Much less is known about a possible role for cAMP-dependent phosphorylation of S163 as a regulator of T cells though one would predict that activation of the enzyme would be consistent with an inhibitory effect of PDE 3 plus 4 inhibition on T cell activation. Further studies will be needed to test how much of the inhibitory effect of cAMP on T cell function might be localized to this phosphosite and regulated by a combination of both PDE3 and PDE4.

## Figure 1

## Cyclic AMP Measurements in response to PDE inhibitor treatment

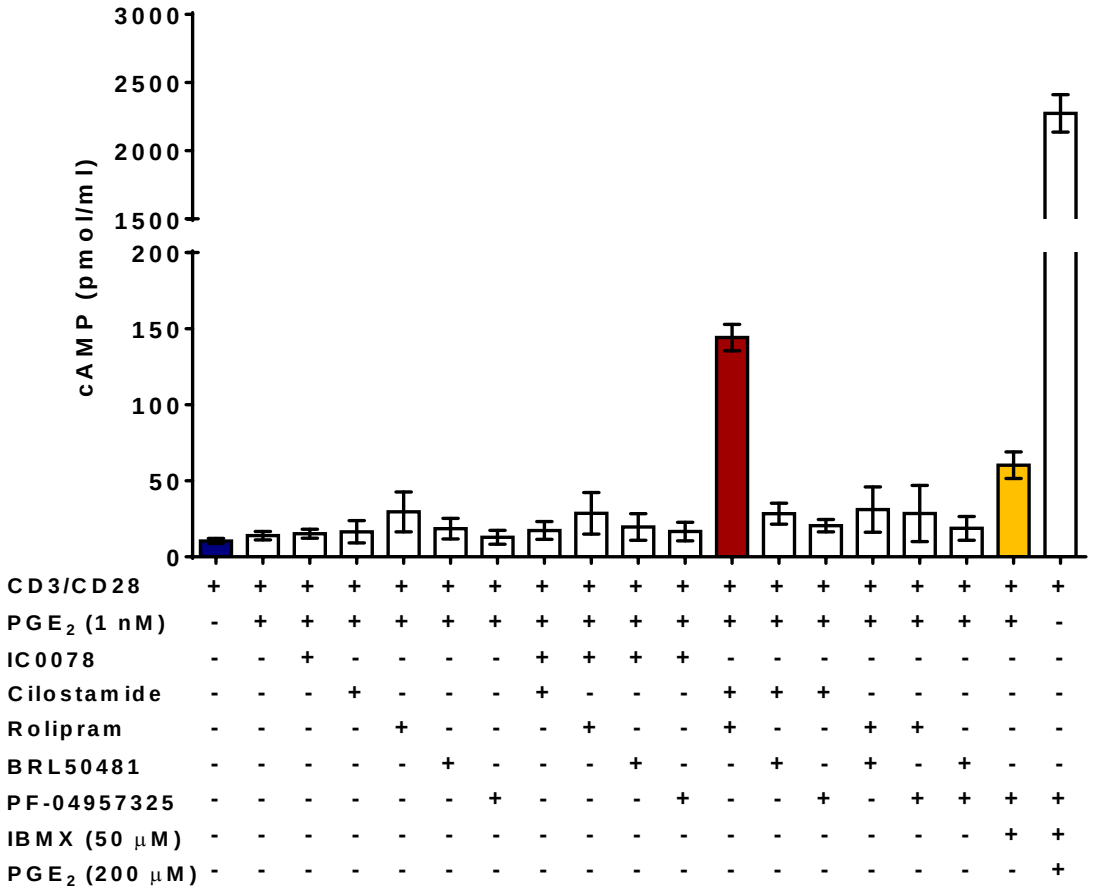


**Fig. 1 – Inhibition of multiple phosphodiesterases is necessary to increase intracellular cAMP.** Jurkat ($1x10^7$) cells were treated as indicated for 20 min. Cells were briefly centrifuged and the supernate discarded. Cell pellets were lysed by adding 1ml of 1:99 mixture of 11.65 M HCL, and 95% EtOH. Pellets were dispersed using a P1000 pipet tip, and vortexed. Lysate was incubated at room temperature for 30 min. Following incubation, the extraction volume was transferred to a fresh microfuge tube, and dried in a speed vac. cAMP was re-suspended in 150 µl of 0.1 M HCl, acetylated, and assayed using a cAMP ELISA kit according to the

manufacturer's recommendations (Cayman Biochemical). Bars are the mean of 3 individual experiments, error bars are std. *Cilostamide and rolipram condition are from 2 indivdual experiments, error bars are the range.

## Figure 2

## Inhibiting multiple PDEs increases both the number and magnitude of phosphorylation changes

**A)**

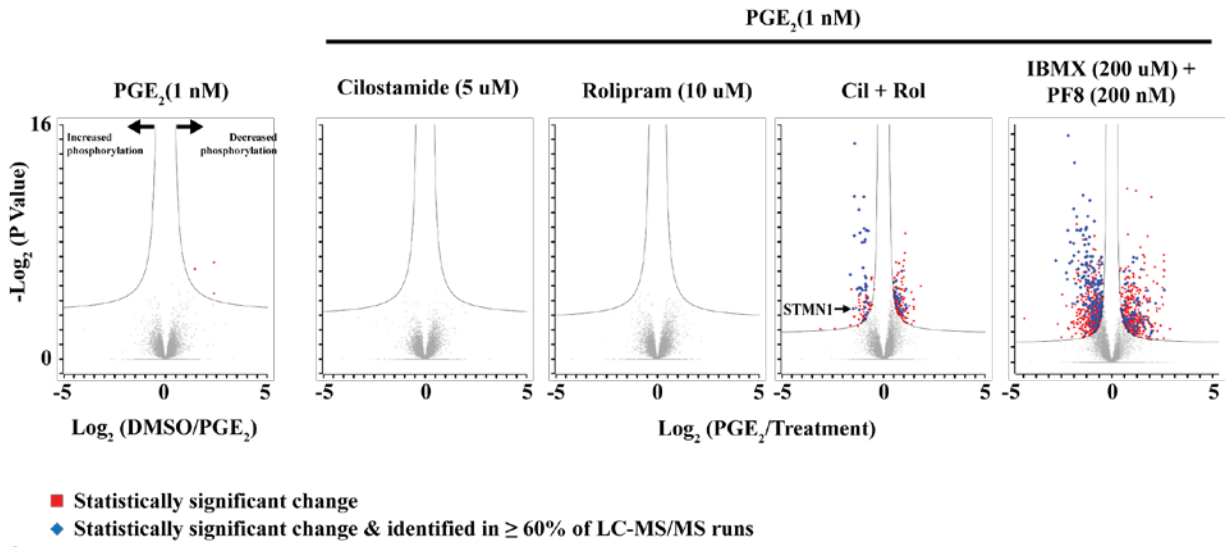


**B)**

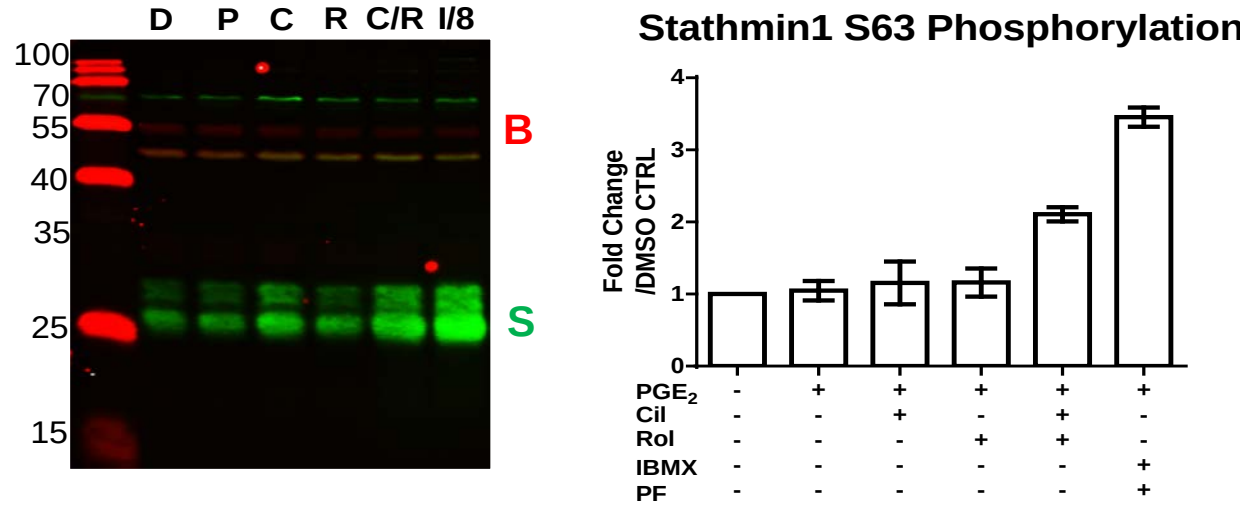


**Fig. 2 Inhibiting multiple PDEs increase the number and magnitude of phosphorylation changes** (A) Volcano plots of the number of phosphosites significantly modulated compared to DMSO as a subset of the total proteome is presented as the log ratio of the DMSO intensity over

the PDE inhibitor intensity plotted against the negative log of the P-value. Red squares are phosphosites significantly modulated over $PGE_2$. Blue diamonds are significantly regulated sites that occur in at least 60% of LC-MS/MS runs. (B) Immunoblot analysis of changes in Stathmin1 phosphorylation at S63. $1x10^7$ cells were treated as previously described. Cells were harvested and boiled in 200 µl Laemmeli buffer and transferred to nitrocellulose. Membranes were probed with anti-Stathmin antibody "S" 1:2000 (Abcam), anti-Beta actin "B" 1:200,000 (Genetex). Membranes were quantified on the Odyssey Scanner Clx (Licor). Blot shown left, and quantified on the right. Bars are mean quantification from 2 experiments. Error bars are the range of two replicates.

## Figure 3

## Distinct regulated phosphopeptides are identified under specific PDE inhibitor treatments

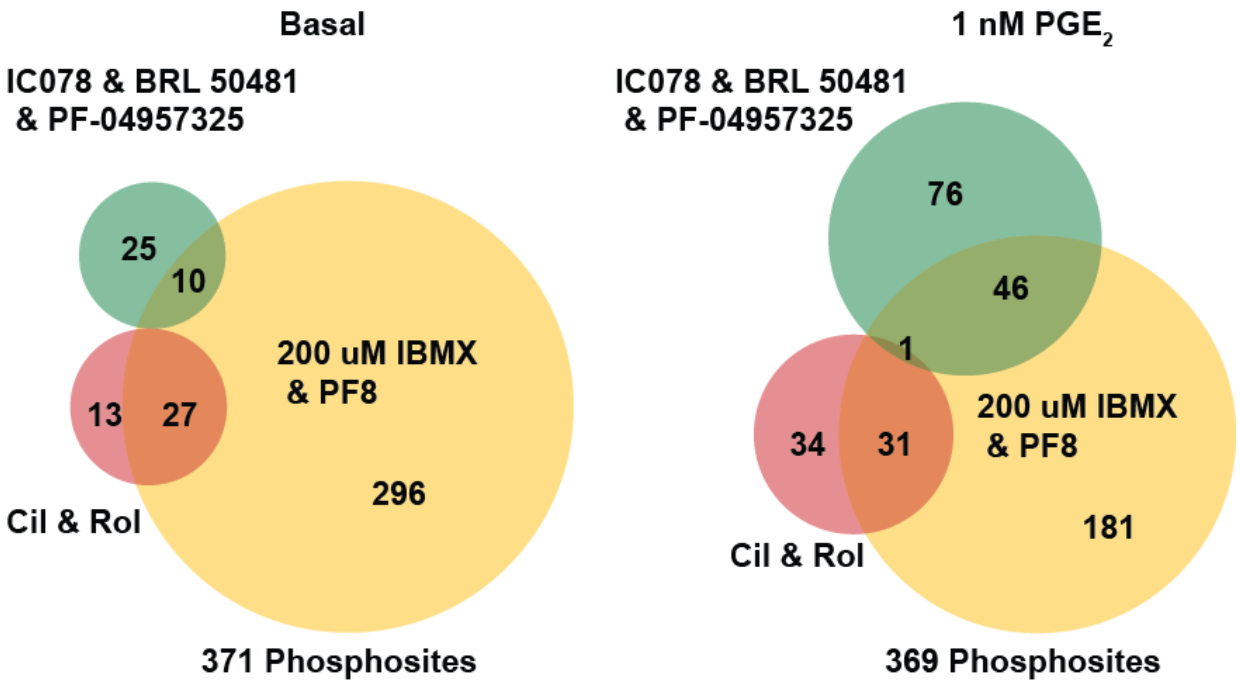


**Fig. 3 - Venn Diagram of number of phosphosites increased by selective PDE inhibition**
Maxquant was used to search mass spectra were searched against the Uniprot human reference proteome, 13,589 phosphopeptides were identified. For further analysis, phosphopeptides must have satisfied the following conditions. First, phosphopeptides must have an intensity value in 60% of the total LC-MS/MS runs in that experimental condition. Second, they must be statistically significant by a two tailed, two sample t-test, multiple comparison correction false discovery rate of 0.05. BioVenn was used to plot the number of unique or common phosphosites identified in each condition(Hulsen, de Vlieg, & Alkema, 2008).

**Figure 4**

**Predicted regulatory kinases of identified phosphosites**

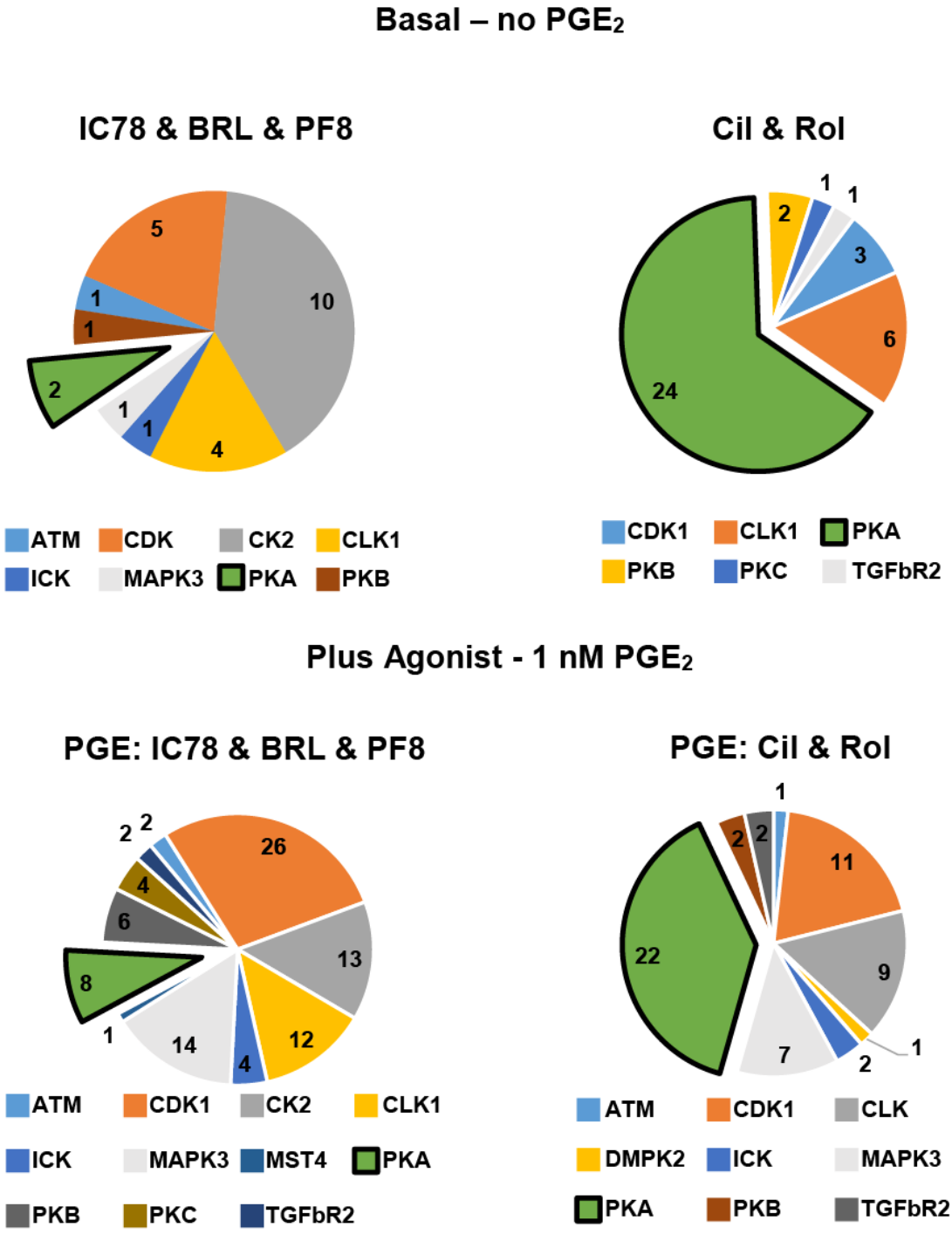

**Fig. 4 - Predicted kinase utilization for different PDE/ agonist combinations** A truncated peptide sequence of 4 amino acid residues flanking the regulated phosphosite was used as an input sequence into NetPhorest to predict kinases responsible for phosphorylating identified sites. Threshold score was set at 0.21.

## Figure 5

## STRING interaction analyses of PDE regulated phosphoproteome

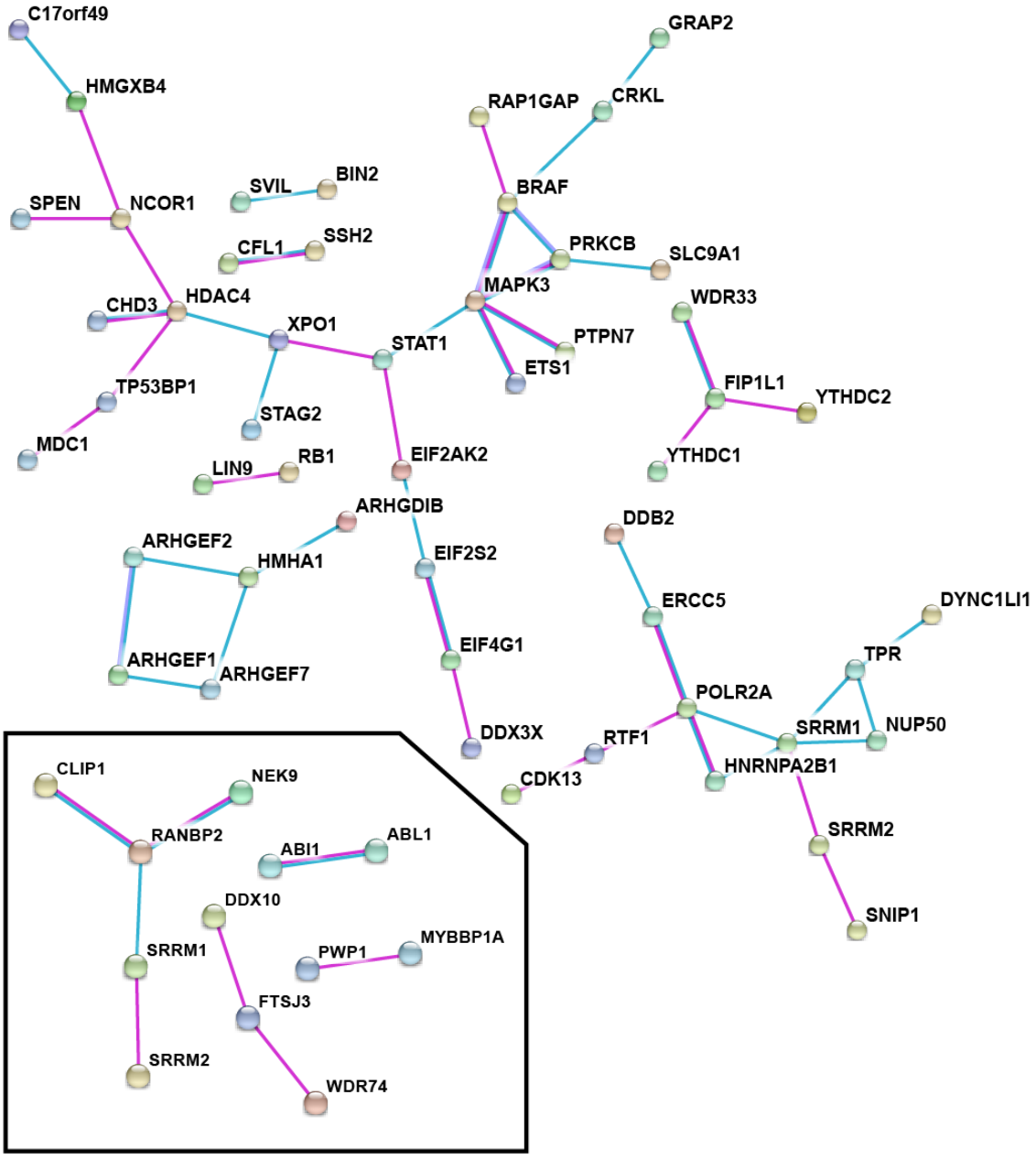


**Fig. 5 – Interaction analysis of proteins with regulated phosphosites by PDEs 1, 7, and 8 inhibitors; and PDE 3 and 4 inhibitor treatment.** A gene list was generated from

phosphosites statistically significantly regulated by PDEs 1, 7, and 8 inhibition; and PDEs 3 and 4 both in the basal and $PGE_2$ stimulated condition. The lists were submitted to the STRING analysis web portal to query the "Experiments" and "Databases" source options, with a minimum interaction score of 0.700. For visual clarity, disconnected nodes were omitted from the interaction map. PDEs 3 and 4 treatment interaction network shown in inset.

## Figure 6

## ClueGo biological process analyses of PDE regulated phosphoproteome

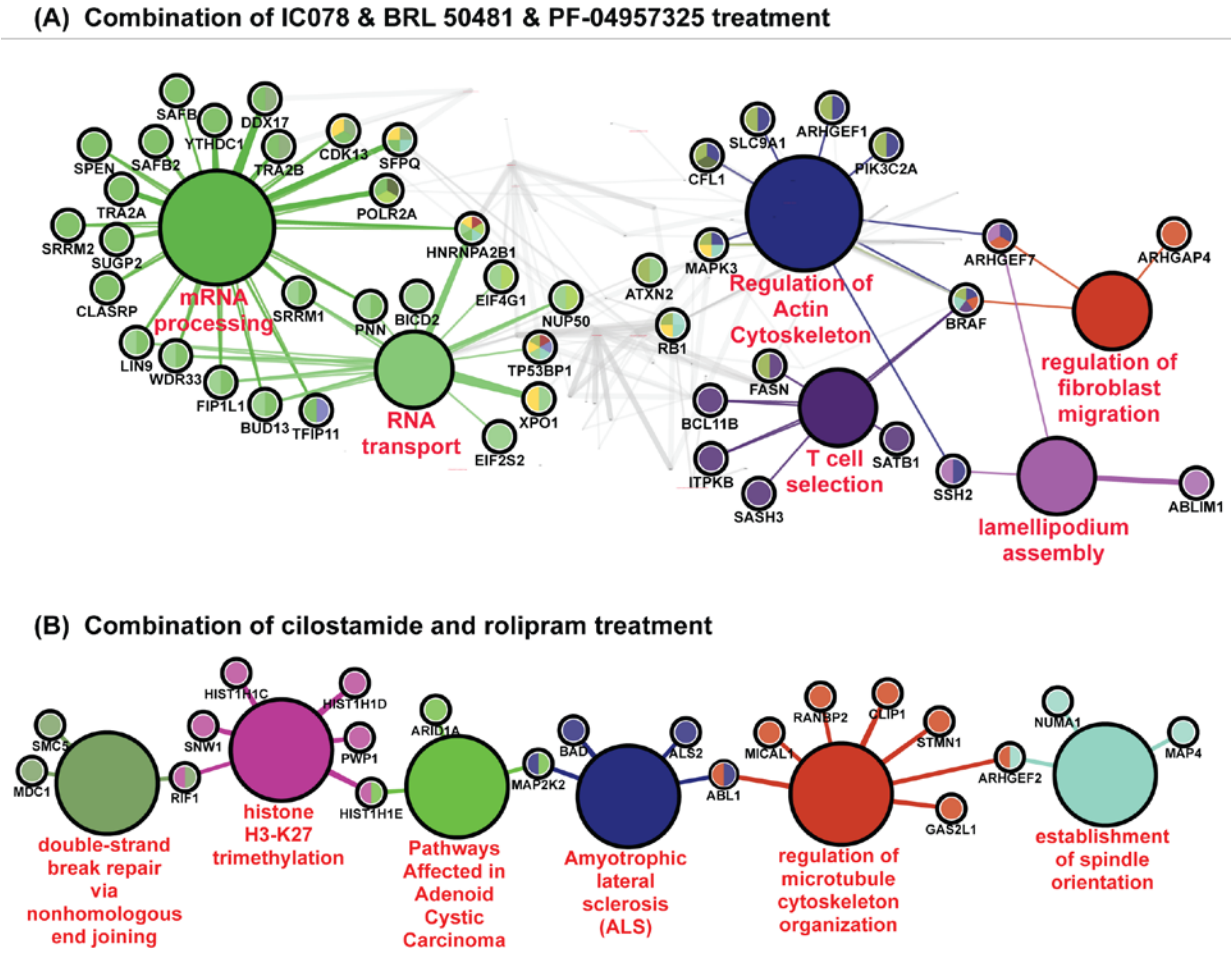


**Fig. 6 - Gene Ontology analysis to identify functional processes regulated by PDE inhibitors.** Gene ontology (GO) analysis was performed using the ClueGo Cytoscape plug in[89]. Lists of unique proteins, for each series of PDE inhibitor treatments (A) combined PDEs 1, 7, and 8 inhibitors—a subset of functions relevant to T cell biology are presented in panel A, the remaining functions are shaded gray. Refer to Supplemental Figure 6 for the full network. (B) combined PDEs 3 and 4 inhibitors were generated from the statistically significantly regulated phosphosites. Each list was used to query the KEGG, Gene Ontology - biological function database, and Wikipathways. ClueGo parameters were set as follows: Go Term Fusion

selected; only display pathways with p values ≤ .05; GO tree interval, all levels; GO term minimum # genes, 3; threshold of 4% of genes per pathway; and kappa score of 0.42. Gene ontology terms are presented as nodes and clustered together based on the similarity of genes present in each term or pathway. Major biological functions are listed in red text. Smaller circles are proteins associated with the adjoining biological process. Circles with multiple colors are associated with more than one processes.

## Table 1

## Top hits for combination of PDEs 1, 7, and 8 inhibitors, basal conditions

| | | | | Fold change over control | | | |
|---|---|---|---|---|---|---|---|
| **Gene** | **Description** | **#** | **Sequence** | **IC, BRL, PF8** | **CIL & ROL** | **IBMX 50μM** | **IBMX 200 μM** |
| ITPKB | Inositol-trisphosphate 3-kinase B | 43 | RAVL**S**PGSV | **3.25** | 1.04 | 1.05 | 3.68 |
| ZC3H15 | Zn Finger CCCH domain containing protein | 381 | NGER**S**DLEE | **2.37** | 0.81 | 0.83 | 0.77 |
| HIRIP3 | HIRA interacting protein 3 | 372 | EVSD**S**EAGG | **2.13** | 1.30 | 1.30 | 1.34 |
| RUNX1 | Runt-related transcription factor 1 | 276 | ATPI**S**PGRA | **1.95** | 1.17 | 0.80 | 1.76 |
| ASUN | Protein asunder homolog | 270 | IIKD**S**PDSP | **1.82** | 1.09 | 0.98 | 1.44 |
| TPR | Nucleoprotein TPR | 2116 | GLQL**T**PGIG | **1.80** | 0.99 | 0.80 | 2.00 |
| HNRN-PA2B1 | Heterogeneous nuclear ribonucleo proteins A2/B1 | 259 | NFGG**S**PGYG | **1.76** | 0.80 | 0.74 | 0.55 |
| RCSD1 | CapZ-interacting protein | 267 | KARR**S**SEEV | **1.68** | 0.92 | 1.00 | 1.34 |
| HDAC4 | Histone deacetylase 4 | 453 | EPIE**S**DEEE | **1.66** | 0.74 | 0.78 | 1.45 |
| PGRMC2 | Membrane-associated progesterone receptor component 2 | 208 | GEEP**S**EYTD | **1.65** | 0.85 | 0.95 | 1.73 |
| SLC9A1 | Sodium/hydrogen exchanger 1 | 796 | QRCL**S**DPGP | **1.57** | 1.12 | 1.10 | 0.85 |
| XPO1 | Exportin-1 | 1055 | KRQM**S**VPGI | **1.57** | 0.00 | 0.00 | 0.97 |

**Legend – Table 1 shows the top 12 phosphorylated proteins in response to combination PDEs 1, 7, and 8 inhibition in the basal condition (no $PGE_2$), compared to changes seen in response to the other PDE inhibitors under the same conditions.** Phosphopeptides containing a consensus PKA primary amino acid phosphorylation sequence are shown in italicized text. Statistically significantly regulated changes in phosphorylation are in bold text.

## Table 2

## Top hits for combination of PDEs 3 and 4 inhibitors, basal conditions

| | | | | Fold change over control | | | |
|---|---|---|---|---|---|---|---|
| **Gene** | **Description** | **#** | **Sequence** | **IC, BRL, PF8** | **CIL & ROL** | **IBMX 50 µM** | **IBMX 200 µM** |
| CAD | CAD protein | 1343 | G*RRL***S**SFVT | 1.10 | **3.31** | **2.80** | **2.86** |
| RANBP2 | E3 SUMO-protein ligase RanBP2 | 1509 | P*RKQ***S**LPAT | 1.30 | **3.17** | 3.98 | **4.23** |
| MAP2K2 | Dual specificity mitogen-activated prot kinase kinase 2 | 394 | NQPG**T**PTRT | 0.37 | **3.01** | 0.34 | 0.44 |
| MAGED2 | Melanoma-associated antigen D2 | 200 | A*RRAS*RGPI | 0.00 | **2.92** | 0.86 | **1.48** |
| HIST1H1E | Histone H1.4; Histone H1.3 | 37 | K*RKAS*GPPV | 1.44 | **2.82** | **3.79** | **4.01** |
| HIST1H1C | Histone H1.2 | 36 | P*RKAS*GPPV | 0.89 | **2.80** | **2.37** | **2.61** |
| UBE2O | E2/E3 hybrid ubiquitin-protein ligase UBE2O | 515 | S*RKKS*IPLS | 0.66 | **2.52** | **1.93** | **0.95** |
| RCSD1 | CapZ-interacting protein | 108 | ASPK**S**PGLK | 1.54 | **2.27** | 0.69 | 1.05 |
| ATAD2 | ATPase family AAA domain-containing protein 2 | 1302 | RARR**S**QVEQ | 1.24 | **2.23** | **3.53** | **3.92** |
| SEC22B | Vesicle-trafficking protein SEC22b | 137 | RNLG**S**INTE | 1.21 | **2.16** | **2.68** | **2.89** |
| GAS2L1 | GAS2-like protein 1 | 316 | ERRG**S**RPEM | 1.25 | **2.15** | 2.32 | 1.67 |
| SSH2 | Protein phosphatase Slingshot homolog 2 | 811 | P*KKNS*IHEL | 1.41 | **2.13** | 1.87 | **2.19** |

**Legend – Table 2 shows the top 12 phosphorylated proteins in response to PDE3 plus 4 inhibition in the basal condition (no $PGE_2$), compared to changes seen in response to the other PDE inhibitors under the same conditions.** Phosphopeptides containing a consensus PKA primary amino acid phosphorylation sequence are shown in italicized text. Statistically significantly regulated changes in phosphorylation are highlighted in bold text.

## Table 3

## Top hits for combination of PDEs 1. 7.and 8 inhibitors, + $PGE_2$

| | | | | Fold change over control | | | |
|---|---|---|---|---|---|---|---|
| **Gene** | **Description** | **#** | **Sequence** | **IC, BRL, PF8** | **CIL & ROL** | **IBMX 50 µM** | **IBMX 200 µM** |
| ITPKB | Inositol-trisphosphate 3-kinase B | 43 | RAVL**S**PGSV | **2.33** | 0.00 | 0.81 | 2.26 |
| ITPKB | Inositol-trisphosphate 3-kinase B | 49 | GSVF**S**PGRG | **2.33** | 0.00 | 0.81 | 2.26 |
| RMDN3 | Reg. of microtubule dynamics prot 3 | 46 | GRSQ**S**LPNS | **2.00** | 1.56 | 1.98 | **1.97** |
| ASUN | Protein asunder homolog | 270 | IIKD**S**PDSP | **2.00** | 0.83 | 1.26 | **1.20** |
| FASN | Fatty acid synthase | 2204 | LACP**T**PKED | **1.91** | 1.02 | 1.09 | **1.42** |
| LASP1 | LIM and SH3 domain protein 1 | 146 | E*RRDS*QDGS | **1.87** | 1.00 | **3.14** | **3.56** |
| ETS1 | Protein C-ets-1 | 285 | PSYD**S**FDSE | **1.84** | 1.27 | 1.23 | 1.19 |
| CDK13 | Cyclin-dependent kinase 13 | 1147 | TDPS**T**PQQE | **1.84** | 1.00 | 1.20 | 1.56 |
| UNG | Uracil-DNA glycosylase | 42 | TSEG**S**DIES | **1.80** | 0.68 | 1.66 | 1.72 |
| HDAC4 | La-related protein 7 | 39 | SRPT**S**EGSD | **1.73** | 0.55 | 1.29 | 1.67 |
| SSH2 | Prot. phosphatase Slingshot homolog 2 | 811 | P*KKNS*IHEL | **1.70** | **2.17** | **2.31** | **2.47** |

**Legend – Table 3 shows the top 11 phosphorylated proteins in response to combination PDEs 1, 7, and 8 inhibition in presence of 1 nM $PGE_2$ compared to changes seen in response to the other PDE inhibitors under the same conditions.** Phosphopeptides containing a consensus PKA primary amino acid phosphorylation sequence are shown in italicized text. Statistically significantly regulated changes in phosphorylation are highlighted in bold text.

## Table 4

## Top hits for combination of PDEs 3 and 4, + $PGE_2$ conditions

| | | | | Fold change over control | | | |
|---|---|---|---|---|---|---|---|
| **Gene** | **Description** | **#** | **Sequence** | **IC, BRL, PF8** | **CIL & ROL** | **IBMX 50 µM** | **IBMX 200 µM** |
| RANBP2 | E3 SUMO-protein ligase RanBP2 | 1509 | P*RKQ***S**LPAT | 2.20 | **4.51** | **5.01** | **5.21** |
| HIST1H1C | Histone H1.2 | 36 | P*RKA***S**GPPV | 1.23 | **4.05** | **3.23** | **3.88** |
| MAGED2 | Melanoma-associated antigen D2 | 200 | A*RRA***S**RGPI | 0.68 | **3.84** | 1.02 | 1.53 |
| SEC22B | Vesicle-trafficking protein SEC22b | 137 | RNLG**S**INTE | 1.44 | **3.36** | **3.45** | **3.50** |
| PWP1 | Periodic tryptophan protein 1 homolog | 485 | ARNS**S**ISGP | 1.27 | **3.29** | **4.42** | **3.20** |
| STMN1 | Stathmin | 63 | E*RRK***S**HEAE | 0.42 | **3.25** | 1.57 | 1.59 |
| HIST1H1E | Histone H1.4 | 37 | K*RKA***S**GPPV | 1.94 | **3.17** | **5.58** | **5.42** |
| NUMA1 | Nuclear mitotic apparat prot1 | 1955 | L*RRA***S**MQPI | 1.49 | **2.91** | **3.59** | **3.59** |
| NFRKB | Nuclear factor related to kappa-B-BP | 310 | G*RKG***S**LAAL | 1.28 | **2.88** | 2.17 | **2.33** |
| CAD | CAD protein;Dihydroorotase | 1343 | G*RRL***S**SFVT | 1.41 | **2.87** | **5.24** | **4.13** |
| MKI67 | Antigen KI-67 | 538 | T*KRK***S**LVMH | 1.14 | **2.53** | **3.25** | **3.02** |

**Legend – Table 4 shows the top 11 phosphorylated proteins in response to PDEs 3 plus 4 inhibition in presence of 1 nM $PGE_2$ compared to changes seen in response to the other PDE inhibitors under the same conditions.** Phosphopeptides containing a consensus PKA primary amino acid phosphorylation sequence are shown in italicized text. Statistically significantly regulated changes in phosphorylation are highlighted in bold.

## Table 5.

## Examples of regulated sites with reported function

| | | | | Predictive Models | | | | |
|---|---|---|---|---|---|---|---|---|
| **Gene** | **Description** | **AA** | **#** | **B** | **L** | **M** | **R** | **RP** |
| LASP1 | LIM and SH3 domain protein 1 | S | 146 | - | - | - | - | + |
| ARHGEF2 | Rho guanine nucleotide exchange factor 2 | S | 858 | - | - | + | - | + |
| PTPN7 | Tyrosine-protein phosphatase non-receptor type 7 | S | 125 | + | + | + | + | + |
| BRAF | Serine/threonine-protein kinase B-raf | S | 446 | + | + | + | + | + |
| NOP58 | Nucleolar protein 58 | S | 502 | - | - | - | - | + |
| NUP50 | Nuclear pore complex prot Nup50 | S | 287 | - | - | - | - | + |
| RAB3IP | Rab-3A-interacting protein | S | 162 | - | - | - | - | + |
| BAD | Bcl2-associated agonist of cell death | S | 74/75 | + | - | - | + | + |
| PGRMC1 | Memb-assoc progest receptor component 1 | S | 57 | - | - | - | - | + |
| STAT1 | Signal transducer and activator of transcription 1-$\alpha/\beta$ | S | 727 | - | + | + | + | + |
| SLC9A1 | Sodium/hydrogen exchanger 1 | S | 796 | - | - | - | + | + |
| SP1 | Transcription factor Sp1 | S | 7 | + | + | + | + | + |
| PRKCB | Protein kinase C beta type | S | 660 | - | + | + | - | + |
| TBC1D1 | TBC1 domain family member 1 | T | 596 | + | + | + | + | + |
| ETS1 | Protein C-ets-1 | S | 282 | + | - | + | + | + |
| PPP1R2 | Protein phosphatase inhibitor 2 | S | 121 | + | + | + | + | + |
| PPP1R2 | Protein phosphatase inhibitor 2 | S | 122 | + | + | + | + | + |
| HMGA1 | High mobility group protein HMG-I/HMG-Y | T | 53 | - | - | - | - | + |
| STMN1 | Stathmin | S | 63 | + | - | - | - | + |
| CAD | CAD protein | S | 1343 | + | + | + | + | + |
| CAMKK1 | Calcium/calmodulin-dependent protein kinase kinase 1 | S | 485 | - | - | - | - | + |
| USP20 | Ubiquitin carboxyl-term hydrolase 20 | S | 333 | - | - | - | - | + |

**Legend – Table 5: Examples of identified proteins with reported regulatory phosphosites**. A truncated peptide sequence of 4 amino acid residues flanking the regulated phosphosite was used to screen the PFP proteomic database for predicted functional phosphosites. Empirically determined regulatory sites (RP) from the PFP database are reported. Predictive models used by PFP are (B)ayes, (L)ogistic, (M)ultilayer, and (R)andom.

## Table 6.

## Examples of PDE IC0078 + BRL50481 + PF-04957325 regulated sites with predicted function

| | | | | | Predictive Models | | | |
|---|---|---|---|---|---|---|---|---|
| **Gene** | **Description** | **AA** | **#** | **Predicted Kinase** | **B** | **L** | **M** | **R** |
| ETS1 | Protein C-ets-1 | S | 285 | # N/A | + | - | + | + |
| HDAC4 | Histone deacetylase 4 | S | 453 | CK2alpha | - | - | - | + |
| RB1 | Retinoblastoma-associated protein | S | 624 | #N/A | + | + | + | + |
| ANAPC2 | Anaphase-promoting complex subunit 2 | S | 314 | MOK | + | + | + | + |
| HIST1H1B | Histone H1.5 | S | 18 | #N/A | + | - | - | - |
| NBEAL2 | Neurobeachin-like protein 2 | T | 1683 | #N/A | - | - | + | - |
| TP53BP1 | Tumor suppressor p53-binding prot 1 | S | 552 | MAPK1 | + | + | + | + |
| BCL11B | B-cell lymphoma/ leukemia 11B | T | 131 | CDK2 | - | - | + | - |

**Legend – Table 6: Examples of proteins with potential regulatory phosphosites modulated by PDE1, 7, and 8 inhibition.** Table 6 shows A truncated peptide sequence of 4 amino acid residues flanking the regulated phosphosite was used to screen the PFP proteomic database for predicted functional phosphosites. Sites were considered positive if at least one of four prediction models suggested function. Predictive models used by PFP are (B)ayes, (L)ogistic, (M)ultilayer, and (R)andom. The same sequence was used in NetPhorest to predict the regulatory kinase. Threshold set at 0.21.

## Table 7.

## Examples of Cilostamide and Rolipram regulated sites with predicted function

| | | | | | Predictive Models | | | |
|---|---|---|---|---|---|---|---|---|
| **Gene** | **Description** | **AA** | **#** | **Predicted Kinase** | **B** | **L** | **M** | **R** |
| NUMA1 | Nuclear mitotic apparatus protein 1 | S | 1955 | #N/A | + | + | + | + |
| MKI67 | Antigen KI-67 | S | 538 | PKAalpha | - | - | + | - |
| NUMA1 | Nuclear mitotic apparatus protein 1 | S | 2033 | #N/A | - | - | - | + |
| FLNA | Filamin-A | T | 2309 | CLK2 | + | + | - | + |
| ATG16L1 | Autophagy-related protein 16-1 | S | 269 | ATM | - | + | + | - |
| PLEKHF2 | Pleckstrin homology domain-containing family F member 2 | S | 16 | PKAalpha | - | - | + | - |
| TEX2 | Testis-expressed sequence 2 protein | S | 295 | PKAalpha | - | + | + | - |
| ABL1 | Tyrosine-protein kinase ABL1 | S | 16 | PKAalpha | - | - | + | - |
| RIF1 | Telomere-associated protein RIF1 | S | 2205 | PKAalpha | + | + | - | + |
| SNX1 | Sorting nexin-1 | S | 188 | PKAalpha | - | + | - | + |
| CUL4A | Cullin-4A | S | 10 | PKAalpha | + | - | - | - |
| PRKDC | DNA-dependent protein kinase catalytic subunit | S | 893 | PKAgamma | + | + | - | + |
| CAMKK2 | Calcium/calmodulin-dependent protein kinase kinase 2 | S | 468 | #N/A | - | - | - | + |
| CDCA2 | Cell division cycle-associated protein 2 | S | 962 | PKAalpha | + | - | - | - |
| MACF1 | Microtubule-actin cross-linking factor 1, isoforms 1/2/3/5 | S | 7068 | #N/A | - | - | + | - |

**Legend- Table 7: Examples of proteins with potential regulatory phosphosites modulated by PDE3, and 8 inhibition** A Truncated peptide sequence of 4 amino acid residues flanking the regulated phospho-site was used to screen the PFP proteomic database for predicted functional phosphosites. Sites were considered positive if at least one of four prediction models suggested function. Predictive models used by PFP are (B)ayes, (L)ogistic, (M)ultilayer, and (R)andom. The same sequence was used in NetPhorest to predict the regulatory kinase. Threshold set at 0.21.

# Chapter 3

# Concluding Remarks

The combined approach of using selective inhibitors with phosphoproteomic analysis builds upon previous classical and phosphoproteomic studies (Giansanti et al., 2013) in several key aspects. Firstly, the majority of previous phosphoproteomic studies used high concentrations of agents such as cAMP analogs or receptor agonists to globally increase cAMP. In others, relatively non-selective phosphatase inhibitors were utilized. In general, the investigators in these studies were most interested in defining a maximal "cAMP-regulated or phosphatase-regulated phosphoproteome". Our data indicate that a much more nuanced understanding, particularly with regards to the physiolological roles for different subsets of PDEs, can be created by using selective PDE inhibitors at their selective concentrations to interrogate the phosphoproteome of a cell.

Secondly, using this combination approach, we have identified a number of proteins known to be key regulators of important pathways/processes that have been largely understudied in the context of cAMP regulation. For example, as also seen in our recent description of a PDE-regulated phosphoproteome of MA-10 cells(Golkowski et al., 2016), a number of small G-protein regulated pathways were identified. As in the MA-10 system, it appears, that the regulation of these pathways is likely to be at the level of the GEFs and GAPs that modulate the small Rho-type GTPases rather than a direct phosphorylation of the GTPase itself. In both studies, inhibition of a combination of PDEs increased ARHGEF2 phosphorylation on S886. This site has been previously reported to regulate ARHGEF2 activity(Meiri et al., 2009). Moreover, ARHGEF2-dependent RhoA activity has also been shown to regulate the uropod of

migrating T cells(Heasman & Ridley, 2010). This is consistent with Vang et al.'s(Vang et al., 2010) report that PDE8 inhibition caused a decrease in T cell motility. In the current study, it was the combination of PDEs 1, 7, and 8 that increased ARHGEF2 phosphorylation. In the context of T cell biology, cytoskeletal reorganization has been intimately linked with T cell receptor signaling. The increased phosphorylation of ABLIM1, ARHGEF1, ARHGEF7, ARHGAP4, BRAF, CFL1, MAPK3, PIK3C2A, SLC9A1, and SSH2 (all proteins associated with cytoskeletal reorganization), suggested that PDE8, possibly in combination with another PDE (likely PDE7) may regulate T cell migration at multiple points (see supplemental material for further discussion of other PDE modulated functional compartments). However, further studies would be necessary to prove this hypothesis.

Finally, we identified a number of PDE-modulated phosphosites on proteins not previously known to be regulated by cAMP/PDEs. For example, RANBP2 was identified as a novel EPAC1 interactor. Gloerich et al. showed that EPAC1 bound to RAN-GTP, which in turn bound to the cluster of zinc finger domains of RANBP2.(Gloerich et al., 2011) They also showed that phosphatase inhibitor treatment increased the phosphorylation of RANBP2 zinc finger domains and prevented EPAC binding. However, the exact site/ zinc finger domain was not identified. PDEs 3 and 4 inhibition caused a significant increase in RANBP2, S1509 phosphorylation (Tables 2 and 4), both under basal and $PGE_2$ conditions. S1509 is immediately C-terminal of the third zinc finger domain, and is within a canonical PKA consensus sequence. It is therefore likely that PKA phosphorylates RANBP2 at S1509 and disrupts RAN-GTP/EPAC binding to the third zinc finger domain. Again, further studies will be necessary to prove this.

Currently, we do not know how many functional PDE-regulated cAMP compartments exist in Jurkat cells. Nor do we understand if similar functional PDE-regulated cGMP pools

exist in these cells. We also need to know if these cyclic nucleotide pools regulate one another and what biological processes each of these functional pools control. The answers to these questions will undoubtedly be complex, and assuredly will be cell context and time dependent. However, this combined selective PDE inhibitor, coupled to phosphoproteomic analysis, is well within current abilities to address these questions. The volume of data to be gleaned is staggering, but with enough experimental iterations it should be possible to construct a "functional atlas", using phosphosites as molecular signatures, of PDE-regulated cyclic nucleotide signaling not only in Jurkat cells, but for any other model cell culture system. Using other agonists and antagonists, the same approach should be possible for the cyclic nucleotide synthetic pathways.

# Bibliography


Abboud, H. E. (1993). Growth factors in glomerulonephritis. *Kidney Int, 43*(1), 252-267.

Abrahamsen, H., Baillie, G., Ngai, J., Vang, T., Nika, K., Ruppelt, A., . . . Tasken, K. (2004). TCR- and CD28-mediated recruitment of phosphodiesterase 4 to lipid rafts potentiates TCR signaling. *J Immunol, 173*(8), 4847-4858.

Aksaas, A. K., Eikvar, S., Akusjarvi, G., Skalhegg, B. S., & Kvissel, A. K. (2011). Protein kinase a-dependent phosphorylation of serine 119 in the proto-oncogenic serine/arginine-rich splicing factor 1 modulates its activity as a splicing enhancer protein. *Genes Cancer, 2*(8), 841-851. doi:10.1177/1947601911430226

Baillie, G. S. (2009). Compartmentalized signalling: spatial regulation of cAMP by the action of compartmentalized phosphodiesterases. *FEBS J, 276*(7), 1790-1799. doi:10.1111/j.1742-4658.2009.06926.x

Baldanzi, G., Bettio, V., Malacarne, V., & Graziani, A. (2016). Diacylglycerol Kinases: Shaping Diacylglycerol and Phosphatidic Acid Gradients to Control Cell Polarity. *Front Cell Dev Biol, 4*, 140. doi:10.3389/fcell.2016.00140

Beretta, L., Dobransky, T., & Sobel, A. (1993). Multiple phosphorylation of stathmin. Identification of four sites phosphorylated in intact cells and in vitro by cyclic AMP-dependent protein kinase and p34cdc2. *J Biol Chem, 268*(27), 20076-20084.

Berthet, J., Rall, T. W., & Sutherland, E. W. (1957). The relationship of epinephrine and glucagon to liver phosphorylase. IV. Effect of epinephrine and glucagon on the reactivation of phosphorylase in liver homogenates. *J Biol Chem, 224*(1), 463-475.

Bindea, G., Mlecnik, B., Hackl, H., Charoentong, P., Tosolini, M., Kirilovsky, A., . . . Galon, J. (2009). ClueGO: a Cytoscape plug-in to decipher functionally grouped gene ontology and pathway annotation networks. *Bioinformatics, 25*(8), 1091-1093. doi:10.1093/bioinformatics/btp101

Bloom, T. J., & Beavo, J. A. (1996). Identification and tissue-specific expression of PDE7 phosphodiesterase splice variants. *Proc Natl Acad Sci U S A, 93*(24), 14188-14192.

Boniface, K., Bak-Jensen, K. S., Li, Y., Blumenschein, W. M., McGeachy, M. J., McClanahan, T. K., . . . de Waal Malefyt, R. (2009). Prostaglandin E2 regulates Th17 cell

differentiation and function through cyclic AMP and EP2/EP4 receptor signaling. *J Exp Med, 206*(3), 535-548. doi:10.1084/jem.20082293

Bozza, P. T., Payne, J. L., Goulet, J. L., & Weller, P. F. (1996). Mechanisms of platelet-activating factor-induced lipid body formation: requisite roles for 5-lipoxygenase and de novo protein synthesis in the compartmentalization of neutrophil lipids. *J Exp Med, 183*(4), 1515-1525.

Brand, C. S., Sadana, R., Malik, S., Smrcka, A. V., & Dessauer, C. W. (2015). Adenylyl Cyclase 5 Regulation by Gbetagamma Involves Isoform-Specific Use of Multiple Interaction Sites. *Mol Pharmacol, 88*(4), 758-767. doi:10.1124/mol.115.099556

Brown, W. S., Khalili, J. S., Rodriguez-Cruz, T. G., Lizee, G., & McIntyre, B. W. (2014). B-Raf regulation of integrin alpha4beta1-mediated resistance to shear stress through changes in cell spreading and cytoskeletal association in T cells. *J Biol Chem, 289*(33), 23141-23153. doi:10.1074/jbc.M114.562918

Builder, S. E., Beavo, J. A., & Krebs, E. G. (1980). Stoichiometry of cAMP and 1,N6-etheno-cAMP binding to protein kinase. *J Biol Chem, 255*(6), 2350-2354.

Butt, E., Gambaryan, S., Gottfert, N., Galler, A., Marcus, K., & Meyer, H. E. (2003). Actin binding of human LIM and SH3 protein is regulated by cGMP- and cAMP-dependent protein kinase phosphorylation on serine 146. *J Biol Chem, 278*(18), 15601-15607. doi:10.1074/jbc.M209009200

Buxton, I. L., & Brunton, L. L. (1983). Compartments of cyclic AMP and protein kinase in mammalian cardiomyocytes. *J Biol Chem, 258*(17), 10233-10239.

Chen, L., Zhang, J. J., & Huang, X. Y. (2008). cAMP inhibits cell migration by interfering with Rac-induced lamellipodium formation. *J Biol Chem, 283*(20), 13799-13805. doi:10.1074/jbc.M800555200

Chini, C. C., Grande, J. P., Chini, E. N., & Dousa, T. P. (1997). Compartmentalization of cAMP signaling in mesangial cells by phosphodiesterase isozymes PDE3 and PDE4. Regulation of superoxidation and mitogenesis. *J Biol Chem, 272*(15), 9854-9859.

Cho, E. A., Kim, E. J., Kwak, S. J., & Juhnn, Y. S. (2014). cAMP signaling inhibits radiation-induced ATM phosphorylation leading to the augmentation of apoptosis in human lung cancer cells. *Mol Cancer, 13*, 36. doi:10.1186/1476-4598-13-36

Clapier, C. R., & Cairns, B. R. (2009). The biology of chromatin remodeling complexes. *Annu Rev Biochem, 78*, 273-304. doi:10.1146/annurev.biochem.77.062706.153223

Conche, C., Boulla, G., Trautmann, A., & Randriamampita, C. (2009). T cell adhesion primes antigen receptor-induced calcium responses through a transient rise in adenosine 3',5'-cyclic monophosphate. *Immunity, 30*(1), 33-43. doi:10.1016/j.immuni.2008.10.020

Cooper, D. M. (2005). Compartmentalization of adenylate cyclase and cAMP signalling. *Biochem Soc Trans, 33*(Pt 6), 1319-1322. doi:10.1042/BST20051319

Cooper, D. M., & Crossthwaite, A. J. (2006). Higher-order organization and regulation of adenylyl cyclases. *Trends Pharmacol Sci, 27*(8), 426-431. doi:10.1016/j.tips.2006.06.002

Corbin, J. D., Sugden, P. H., Lincoln, T. M., & Keely, S. L. (1977). Compartmentalization of adenosine 3':5'-monophosphate and adenosine 3':5'-monophosphate-dependent protein kinase in heart tissue. *J Biol Chem, 252*(11), 3854-3861.

Cox, J., & Mann, M. (2008). MaxQuant enables high peptide identification rates, individualized p.p.b.-range mass accuracies and proteome-wide protein quantification. *Nat Biotechnol, 26*(12), 1367-1372. doi:10.1038/nbt.1511

Cruz-Garcia, D., Ortega-Bellido, M., Scarpa, M., Villeneuve, J., Jovic, M., Porzner, M., . . . Malhotra, V. (2013). Recruitment of arfaptins to the trans-Golgi network by PI(4)P and their involvement in cargo export. *EMBO J, 32*(12), 1717-1729. doi:10.1038/emboj.2013.116

de Graaf, E. L., Giansanti, P., Altelaar, A. F., & Heck, A. J. (2014). Single-step enrichment by Ti4+-IMAC and label-free quantitation enables in-depth monitoring of phosphorylation dynamics with high reproducibility and temporal resolution. *Mol Cell Proteomics, 13*(9), 2426-2434. doi:10.1074/mcp.O113.036608

de Rooij, J., Rehmann, H., van Triest, M., Cool, R. H., Wittinghofer, A., & Bos, J. L. (2000). Mechanism of regulation of the Epac family of cAMP-dependent RapGEFs. *J Biol Chem, 275*(27), 20829-20836. doi:10.1074/jbc.M001113200

de Rooij, J., Zwartkruis, F. J., Verheijen, M. H., Cool, R. H., Nijman, S. M., Wittinghofer, A., & Bos, J. L. (1998). Epac is a Rap1 guanine-nucleotide-exchange factor directly activated by cyclic AMP. *Nature, 396*(6710), 474-477. doi:10.1038/24884

DiFrancesco, D., & Tortora, P. (1991). Direct activation of cardiac pacemaker channels by intracellular cyclic AMP. *Nature, 351*(6322), 145-147. doi:10.1038/351145a0

Dodge, K. L., Khouangsathiene, S., Kapiloff, M. S., Mouton, R., Hill, E. V., Houslay, M. D., . . . Scott, J. D. (2001). mAKAP assembles a protein kinase A/PDE4 phosphodiesterase cAMP signaling module. *EMBO J, 20*(8), 1921-1930. doi:10.1093/emboj/20.8.1921

Dong, H. L., Zitt, C., Auriga, C., Hatzelmann, A., & Epstein, P. M. (2010). Inhibition of PDE3 PDE4 and PDE7 potentiates glucocorticoid-induced apoptosis and overcomes glucocorticoid resistance in CEM T leukemic cells. *Biochemical Pharmacology, 79*(3), 321-329. doi:10.1016/j.bcp.2009.09.001

Downes, G. B., & Gautam, N. (1999). The G protein subunit gene families. *Genomics, 62*(3), 544-552. doi:10.1006/geno.1999.5992

Eliezer, Y., Argaman, L., Kornowski, M., Roniger, M., & Goldberg, M. (2014). Interplay between the DNA damage proteins MDC1 and ATM in the regulation of the spindle assembly checkpoint. *J Biol Chem, 289*(12), 8182-8193. doi:10.1074/jbc.M113.532739

Erdogan, S., & Houslay, M. D. (1997). Challenge of human Jurkat T-cells with the adenylate cyclase activator forskolin elicits major changes in cAMP phosphodiesterase (PDE) expression by up-regulating PDE3 and inducing PDE4D1 and PDE4D2 splice variants as well as down-regulating a novel PDE4A splice variant. *Biochem J, 321 ( Pt 1)*, 165-175.

Erlichman, J., Rubin, C. S., & Rosen, O. M. (1973). Physical properties of a purified cyclic adenosine 3':5'-monophosphate-dependent protein kinase from bovine heart muscle. *J Biol Chem, 248*(21), 7607-7609.

Feng, G., Yan, Z., Li, C., & Hou, Y. (2016). microRNA-208a in an early stage myocardial infarction rat model and the effect on cAMP-PKA signaling pathway. *Mol Med Rep, 14*(2), 1631-1635. doi:10.3892/mmr.2016.5402

Fesenko, E. E., Kolesnikov, S. S., & Lyubarsky, A. L. (1985). Induction by cyclic GMP of cationic conductance in plasma membrane of retinal rod outer segment. *Nature, 313*(6000), 310-313.

Franciosi, L. G., Diamant, Z., Banner, K. H., Zuiker, R., Morelli, N., Kamerling, I. M., . . . Page, C. P. (2013). Efficacy and safety of RPL554, a dual PDE3 and PDE4 inhibitor, in healthy volunteers and in patients with asthma or chronic obstructive pulmonary disease: findings

from four clinical trials. *Lancet Respir Med, 1*(9), 714-727. doi:10.1016/S2213-2600(13)70187-5

Gehart, H., Goginashvili, A., Beck, R., Morvan, J., Erbs, E., Formentini, I., . . . Ricci, R. (2012). The BAR domain protein Arfaptin-1 controls secretory granule biogenesis at the trans-Golgi network. *Dev Cell, 23*(4), 756-768. doi:10.1016/j.devcel.2012.07.019

Gharbi, S. I., Rincon, E., Avila-Flores, A., Torres-Ayuso, P., Almena, M., Cobos, M. A., . . . Merida, I. (2011). Diacylglycerol kinase zeta controls diacylglycerol metabolism at the immunological synapse. *Mol Biol Cell, 22*(22), 4406-4414. doi:10.1091/mbc.E11-03-0247

Gharibi, S., Hajian, M., Ostadhosseini, S., Hosseini, S. M., Forouzanfar, M., & Nasr-Esfahani, M. H. (2013). Effect of phosphodiesterase type 3 inhibitor on nuclear maturation and in vitro development of ovine oocytes. *Theriogenology, 80*(4), 302-312. doi:10.1016/j.theriogenology.2013.04.012

Ghesquiere, B., Jonckheere, V., Colaert, N., Van Durme, J., Timmerman, E., Goethals, M., . . . Gevaert, K. (2011). Redox proteomics of protein-bound methionine oxidation. *Mol Cell Proteomics, 10*(5), M110 006866. doi:10.1074/mcp.M110.006866

Giansanti, P., Stokes, M. P., Silva, J. C., Scholten, A., & Heck, A. J. (2013). Interrogating cAMP-dependent kinase signaling in Jurkat T cells via a protein kinase A targeted immune-precipitation phosphoproteomics approach. *Mol Cell Proteomics, 12*(11), 3350-3359. doi:10.1074/mcp.O113.028456

Giembycz, M. A., Corrigan, C. J., Seybold, J., Newton, R., & Barnes, P. J. (1996). Identification of cyclic AMP phosphodiesterases 3, 4 and 7 in human CD4+ and CD8+ T-lymphocytes: role in regulating proliferation and the biosynthesis of interleukin-2. *Br J Pharmacol, 118*(8), 1945-1958.

Gill, G. N., & Garren, L. D. (1969). On the mechanism of action of adrenocorticotropic hormone: the binding of cyclic-3',5'-adenosine monophosphate to an adrenal cortical protein. *Proc Natl Acad Sci U S A, 63*(2), 512-519.

Gill, G. N., & Garren, L. D. (1971). Role of the receptor in the mechanism of action of adenosine 3':5'-cyclic monophosphate. *Proc Natl Acad Sci U S A, 68*(4), 786-790.

Gloerich, M., Vliem, M. J., Prummel, E., Meijer, L. A., Rensen, M. G., Rehmann, H., & Bos, J. L. (2011). The nucleoporin RanBP2 tethers the cAMP effector Epac1 and inhibits its catalytic activity. *J Cell Biol, 193*(6), 1009-1020. doi:10.1083/jcb.201011126

Gold, M. G., Fowler, D. M., Means, C. K., Pawson, C. T., Stephany, J. J., Langeberg, L. K., . . . Scott, J. D. (2013). Engineering A-kinase anchoring protein (AKAP)-selective regulatory subunits of protein kinase A (PKA) through structure-based phage selection. *J Biol Chem, 288*(24), 17111-17121. doi:10.1074/jbc.M112.447326

Golkowski, M., Shimizu-Albergine, M., Suh, H. W., Beavo, J. A., & Ong, S. E. (2016). Studying mechanisms of cAMP and cyclic nucleotide phosphodiesterase signaling in Leydig cell function with phosphoproteomics. *Cell Signal, 28*(7), 764-778. doi:10.1016/j.cellsig.2015.11.014

Gupta, M., George, A., Sen, R., Rath, S., Durdik, J. M., & Bal, V. (1999). Presence of pentoxifylline during T cell priming increases clonal frequencies in secondary proliferative responses and inhibits apoptosis. *J Immunol, 162*(2), 689-695.

Hasler, P., Moore, J. J., & Kammer, G. M. (1992). Human T lymphocyte cAMP-dependent protein kinase: subcellular distributions and activity ranges of type I and type II isozymes. *FASEB J, 6*(9), 2735-2741.

Hayes, J. S., Brunton, L. L., Brown, J. H., Reese, J. B., & Mayer, S. E. (1979). Hormonally specific expression of cardiac protein kinase activity. *Proc Natl Acad Sci U S A, 76*(4), 1570-1574.

Heasman, S. J., & Ridley, A. J. (2010). Multiple roles for RhoA during T cell transendothelial migration. *Small GTPases, 1*(3), 174-179. doi:10.4161/sgtp.1.3.14724

Hedrich, C. M., Crispin, J. C., Rauen, T., Ioannidis, C., Koga, T., Rodriguez Rodriguez, N., . . . Tsokos, G. C. (2014). cAMP responsive element modulator (CREM) alpha mediates chromatin remodeling of CD8 during the generation of CD3+ CD4- CD8- T cells. *J Biol Chem, 289*(4), 2361-2370. doi:10.1074/jbc.M113.523605

Hirsch, A. H., Glantz, S. B., Li, Y., You, Y., & Rubin, C. S. (1992). Cloning and expression of an intron-less gene for AKAP 75, an anchor protein for the regulatory subunit of cAMP-dependent protein kinase II beta. *J Biol Chem, 267*(4), 2131-2134.

Hood, F. E., & Clarke, P. R. (2007). RCC1 isoforms differ in their affinity for chromatin, molecular interactions and regulation by phosphorylation. *J Cell Sci, 120*(Pt 19), 3436-3445. doi:10.1242/jcs.009092

Horiike, Y., Kobayashi, H., & Sekiguchi, T. (2009). Ran GTPase guanine nucleotide exchange factor RCC1 is phosphorylated on serine 11 by cdc2 kinase in vitro. *Mol Biol Rep, 36*(4), 717-723. doi:10.1007/s11033-008-9234-3

Horn, H., Schoof, E. M., Kim, J., Robin, X., Miller, M. L., Diella, F., . . . Linding, R. (2014). KinomeXplorer: an integrated platform for kinome biology studies. *Nat Methods, 11*(6), 603-604. doi:10.1038/nmeth.2968

Hornbeck, P. V., Zhang, B., Murray, B., Kornhauser, J. M., Latham, V., & Skrzypek, E. (2015). PhosphoSitePlus, 2014: mutations, PTMs and recalibrations. *Nucleic Acids Res, 43*(Database issue), D512-520. doi:10.1093/nar/gku1267

Howe, A. K. (2004). Regulation of actin-based cell migration by cAMP/PKA. *Biochim Biophys Acta, 1692*(2-3), 159-174. doi:10.1016/j.bbamcr.2004.03.005

Huang, B., Zhao, J., Lei, Z., Shen, S., Li, D., Shen, G. X., . . . Feng, Z. H. (2009). miR-142-3p restricts cAMP production in CD4+CD25- T cells and CD4+CD25+ TREG cells by targeting AC9 mRNA. *EMBO Rep, 10*(2), 180-185. doi:10.1038/embor.2008.224

Hulsen, T., de Vlieg, J., & Alkema, W. (2008). BioVenn - a web application for the comparison and visualization of biological lists using area-proportional Venn diagrams. *BMC Genomics, 9*, 488. doi:10.1186/1471-2164-9-488

Hutchins, J. R., Moore, W. J., Hood, F. E., Wilson, J. S., Andrews, P. D., Swedlow, J. R., & Clarke, P. R. (2004). Phosphorylation regulates the dynamic interaction of RCC1 with chromosomes during mitosis. *Curr Biol, 14*(12), 1099-1104. doi:10.1016/j.cub.2004.05.021

Ichiba, T., Hoshi, Y., Eto, Y., Tajima, N., & Kuraishi, Y. (1999). Characterization of GFR, a novel guanine nucleotide exchange factor for Rap1. *FEBS Lett, 457*(1), 85-89.

Ivanov, V. N., Lee, R. K., Podack, E. R., & Malek, T. R. (1997). Regulation of Fas-dependent activation-induced T cell apoptosis by cAMP signaling: a potential role for transcription factor NF-kappa B. *Oncogene, 14*(20), 2455-2464. doi:10.1038/sj.onc.1201088

Jarnaess, E., Stokka, A. J., Kvissel, A. K., Skalhegg, B. S., Torgersen, K. M., Scott, J. D., . . . Tasken, K. (2009). Splicing factor arginine/serine-rich 17A (SFRS17A) is an A-kinase anchoring protein that targets protein kinase A to splicing factor compartments. *J Biol Chem, 284*(50), 35154-35164. doi:10.1074/jbc.M109.056465

Jersie-Christensen, R. R., Sultan, A., & Olsen, J. V. (2016). Simple and Reproducible Sample Preparation for Single-Shot Phosphoproteomics with High Sensitivity. *Methods Mol Biol, 1355*, 251-260. doi:10.1007/978-1-4939-3049-4_17

Jurevicius, J., & Fischmeister, R. (1996). cAMP compartmentation is responsible for a local activation of cardiac Ca2+ channels by beta-adrenergic agonists. *Proc Natl Acad Sci U S A, 93*(1), 295-299.

Kawasaki, H., Springett, G. M., Mochizuki, N., Toki, S., Nakaya, M., Matsuda, M., . . . Graybiel, A. M. (1998). A family of cAMP-binding proteins that directly activate Rap1. *Science, 282*(5397), 2275-2279.

Keely, S. L. (1979). Prostaglandin E1 activation of heart cAMP-dependent protein kinase: apparent dissociation of protein kinase activation from increases in phosphorylase activity and contractile force. *Mol Pharmacol, 15*(2), 235-245.

Kemp, B. E., Benjamini, E., & Krebs, E. G. (1976). Synthetic hexapeptide substrates and inhibitors of 3':5'-cyclic AMP-dependent protein kinase. *Proc Natl Acad Sci U S A, 73*(4), 1038-1042.

Kemp, B. E., Graves, D. J., Benjamini, E., & Krebs, E. G. (1977). Role of multiple basic residues in determining the substrate specificity of cyclic AMP-dependent protein kinase. *J Biol Chem, 252*(14), 4888-4894.

Kotsis, D. H., Masko, E. M., Sigoillot, F. D., Di Gregorio, R., Guy-Evans, H. I., & Evans, D. R. (2007). Protein kinase A phosphorylation of the multifunctional protein CAD antagonizes activation by the MAP kinase cascade. *Mol Cell Biochem, 301*(1-2), 69-81. doi:10.1007/s11010-006-9398-x

Krishna, S., & Zhong, X. (2013). Role of diacylglycerol kinases in T cell development and function. *Crit Rev Immunol, 33*(2), 97-118.

Lai, A. Y., & Wade, P. A. (2011). Cancer biology and NuRD: a multifaceted chromatin remodelling complex. *Nat Rev Cancer, 11*(8), 588-596. doi:10.1038/nrc3091

Lalli, E., Sassone-Corsi, P., & Ceredig, R. (1996). Block of T lymphocyte differentiation by activation of the cAMP-dependent signal transduction pathway. *EMBO J, 15*(3), 528-537.

Li, H., Liu, G., Yu, J., Cao, W., Lobo, V. G., & Xie, J. (2009). In vivo selection of kinase-responsive RNA elements controlling alternative splicing. *J Biol Chem, 284*(24), 16191-16201. doi:10.1074/jbc.M900393200

Li, P., Xue, W. J., Feng, Y., & Mao, Q. S. (2015). MicroRNA-205 functions as a tumor suppressor in colorectal cancer by targeting cAMP responsive element binding protein 1 (CREB1). *Am J Transl Res, 7*(10), 2053-2059.

Li, Y., Asuri, S., Rebhun, J. F., Castro, A. F., Paranavitana, N. C., & Quilliam, L. A. (2006). The RAP1 guanine nucleotide exchange factor Epac2 couples cyclic AMP and Ras signals at the plasma membrane. *J Biol Chem, 281*(5), 2506-2514. doi:10.1074/jbc.M508165200

Li, Y., Deng, C., Hu, X., Patel, B., Fu, X., Qiu, Y., . . . Huang, S. (2012). Dynamic interaction between TAL1 oncoprotein and LSD1 regulates TAL1 function in hematopoiesis and leukemogenesis. *Oncogene, 31*(48), 5007-5018. doi:10.1038/onc.2012.8

Liu, D. T., Tibbs, G. R., Paoletti, P., & Siegelbaum, S. A. (1998). Constraining ligand-binding site stoichiometry suggests that a cyclic nucleotide-gated channel is composed of two functional dimers. *Neuron, 21*(1), 235-248.

Liu, H., & Maurice, D. H. (1998). Expression of cyclic GMP-inhibited phosphodiesterases 3A and 3B (PDE3A and PDE3B) in rat tissues: differential subcellular localization and regulated expression by cyclic AMP. *Br J Pharmacol, 125*(7), 1501-1510. doi:10.1038/sj.bjp.0702227

Lizcano, J. M., Morrice, N., & Cohen, P. (2000). Regulation of BAD by cAMP-dependent protein kinase is mediated via phosphorylation of a novel site, Ser155. *Biochem J, 349*(Pt 2), 547-557.

Marklund, U., Larsson, N., Brattsand, G., Osterman, O., Chatila, T. A., & Gullberg, M. (1994). Serine 16 of oncoprotein 18 is a major cytosolic target for the Ca2+/calmodulin-dependent kinase-Gr. *Eur J Biochem, 225*(1), 53-60.

Mayya, V., Lundgren, D. H., Hwang, S. I., Rezaul, K., Wu, L., Eng, J. K., . . . Han, D. K. (2009). Quantitative phosphoproteomic analysis of T cell receptor signaling reveals system-wide modulation of protein-protein interactions. *Sci Signal, 2*(84), ra46. doi:10.1126/scisignal.2000007

Meiri, D., Greeve, M. A., Brunet, A., Finan, D., Wells, C. D., LaRose, J., & Rottapel, R. (2009). Modulation of Rho guanine exchange factor Lfc activity by protein kinase A-mediated phosphorylation. *Mol Cell Biol, 29*(21), 5963-5973. doi:10.1128/MCB.01268-08

Meiri, D., Marshall, C. B., Greeve, M. A., Kim, B., Balan, M., Suarez, F., . . . Rottapel, R. (2012). Mechanistic insight into the microtubule and actin cytoskeleton coupling through dynein-dependent RhoGEF inhibition. *Mol Cell, 45*(5), 642-655. doi:10.1016/j.molcel.2012.01.027

Mihlan, S., Reiss, C., Thalheimer, P., Herterich, S., Gaetzner, S., Kremerskothen, J., . . . Butt, E. (2013). Nuclear import of LASP-1 is regulated by phosphorylation and dynamic protein-protein interactions. *Oncogene, 32*(16), 2107-2113. doi:10.1038/onc.2012.216

Milo, R. (2013). What is the total number of protein molecules per cell volume? A call to rethink some published values. *Bioessays, 35*(12), 1050-1055. doi:10.1002/bies.201300066

Nakamura, T., & Gold, G. H. (1987). A cyclic nucleotide-gated conductance in olfactory receptor cilia. *Nature, 325*(6103), 442-444. doi:10.1038/325442a0

Nakaya, M., Xiao, Y., Zhou, X., Chang, J. H., Chang, M., Cheng, X., . . . Sun, S. C. (2014). Inflammatory T cell responses rely on amino acid transporter ASCT2 facilitation of glutamine uptake and mTORC1 kinase activation. *Immunity, 40*(5), 692-705. doi:10.1016/j.immuni.2014.04.007

Newsholme, E. A., Crabtree, B., & Ardawi, M. S. (1985). Glutamine metabolism in lymphocytes: its biochemical, physiological and clinical importance. *Q J Exp Physiol, 70*(4), 473-489.

Nguyen, T. D., Carrascal, M., Vidal-Cortes, O., Gallardo, O., Casas, V., Gay, M., . . . Abian, J. (2016). The phosphoproteome of human Jurkat T cell clones upon costimulation with anti-CD3/anti-CD28 antibodies. *J Proteomics, 131*, 190-198. doi:10.1016/j.jprot.2015.10.029

Nika, K., Charvet, C., Williams, S., Tautz, L., Bruckner, S., Rahmouni, S., . . . Mustelin, T. (2006). Lipid raft targeting of hematopoietic protein tyrosine phosphatase by protein kinase C theta-mediated phosphorylation. *Mol Cell Biol, 26*(5), 1806-1816. doi:10.1128/MCB.26.5.1806-1816.2006

Oldham, W. M., & Hamm, H. E. (2008). Heterotrimeric G protein activation by G-protein-coupled receptors. *Nat Rev Mol Cell Biol, 9*(1), 60-71. doi:10.1038/nrm2299

Olmedo, I., Munoz, C., Guzman, N., Catalan, M., Vivar, R., Ayala, P., . . . Diaz-Araya, G. (2013). EPAC expression and function in cardiac fibroblasts and myofibroblasts. *Toxicol Appl Pharmacol, 272*(2), 414-422. doi:10.1016/j.taap.2013.06.022

Omori, K., & Kotera, J. (2007). Overview of PDEs and their regulation. *Circ Res, 100*(3), 309-327. doi:10.1161/01.RES.0000256354.95791.f1

Pereira, L., Rehmann, H., Lao, D. H., Erickson, J. R., Bossuyt, J., Chen, J., & Bers, D. M. (2015). Novel Epac fluorescent ligand reveals distinct Epac1 vs. Epac2 distribution and function in cardiomyocytes. *Proc Natl Acad Sci U S A, 112*(13), 3991-3996. doi:10.1073/pnas.1416163112

Phang, H. Q., Hoon, J. L., Lai, S. K., Zeng, Y., Chiam, K. H., Li, H. Y., & Koh, C. G. (2014). POPX2 phosphatase regulates the KIF3 kinesin motor complex. *J Cell Sci, 127*(Pt 4), 727-739. doi:10.1242/jcs.126482

Ponomarenko, E. A., Poverennaya, E. V., Ilgisonis, E. V., Pyatnitskiy, M. A., Kopylov, A. T., Zgoda, V. G., . . . Archakov, A. I. (2016). The Size of the Human Proteome: The Width and Depth. *Int J Anal Chem, 2016*, 7436849. doi:10.1155/2016/7436849

Poppinga, W. J., Munoz-Llancao, P., Gonzalez-Billault, C., & Schmidt, M. (2014). A-kinase anchoring proteins: cAMP compartmentalization in neurodegenerative and obstructive pulmonary diseases. *Br J Pharmacol, 171*(24), 5603-5623. doi:10.1111/bph.12882

Prasad, K. S., & Brandt, S. J. (1997). Target-dependent effect of phosphorylation on the DNA binding activity of the TAL1/SCL oncoprotein. *J Biol Chem, 272*(17), 11457-11462.

Rall, T. W., & Sutherland, E. W. (1958). Formation of a cyclic adenine ribonucleotide by tissue particles. *J Biol Chem, 232*(2), 1065-1076.

Rappsilber, J., Ishihama, Y., & Mann, M. (2003). Stop and go extraction tips for matrix-assisted laser desorption/ionization, nanoelectrospray, and LC/MS sample pretreatment in proteomics. *Anal Chem, 75*(3), 663-670.

Robison, G. A., Butcher, R. W., & Sutherland, E. W. (1968). Cyclic AMP. *Annu Rev Biochem, 37*, 149-174. doi:10.1146/annurev.bi.37.070168.001053

Salek, M., McGowan, S., Trudgian, D. C., Dushek, O., de Wet, B., Efstathiou, G., & Acuto, O. (2013). Quantitative phosphoproteome analysis unveils LAT as a modulator of CD3zeta

and ZAP-70 tyrosine phosphorylation. *PLoS One, 8*(10), e77423. doi:10.1371/journal.pone.0077423

Saxena, M., Williams, S., Tasken, K., & Mustelin, T. (1999). Crosstalk between cAMP-dependent kinase and MAP kinase through a protein tyrosine phosphatase. *Nat Cell Biol, 1*(5), 305-311. doi:10.1038/13024

Sinha, C., Ren, A., Arora, K., Moon, C. S., Yarlagadda, S., Woodrooffe, K., . . . Naren, A. P. (2015). PKA and actin play critical roles as downstream effectors in MRP4-mediated regulation of fibroblast migration. *Cell Signal, 27*(7), 1345-1355. doi:10.1016/j.cellsig.2015.03.022

Sugimoto, K., Suzuki, H. I., Fujimura, T., Ono, A., Kaga, N., Isobe, Y., . . . Komatsu, N. (2015). A clinically attainable dose of L-asparaginase targets glutamine addiction in lymphoid cell lines. *Cancer Sci, 106*(11), 1534-1543. doi:10.1111/cas.12807

Sutherland, E. W., & Rall, T. W. (1958). Fractionation and characterization of a cyclic adenine ribonucleotide formed by tissue particles. *J Biol Chem, 232*(2), 1077-1091.

Szklarczyk, D., Franceschini, A., Wyder, S., Forslund, K., Heller, D., Huerta-Cepas, J., . . . von Mering, C. (2015). STRING v10: protein-protein interaction networks, integrated over the tree of life. *Nucleic Acids Res, 43*(Database issue), D447-452. doi:10.1093/nar/gku1003

Tran, N. H., Wu, X., & Frost, J. A. (2005). B-Raf and Raf-1 are regulated by distinct autoregulatory mechanisms. *J Biol Chem, 280*(16), 16244-16253. doi:10.1074/jbc.M501185200

Tyanova, S., Temu, T., Sinitcyn, P., Carlson, A., Hein, M. Y., Geiger, T., . . . Cox, J. (2016). The Perseus computational platform for comprehensive analysis of (prote)omics data. *Nat Methods, 13*(9), 731-740. doi:10.1038/nmeth.3901

Vaman, V. S. A., Poppe, H., Houben, R., Grunewald, T. G., Goebeler, M., & Butt, E. (2015). LASP1, a Newly Identified Melanocytic Protein with a Possible Role in Melanin Release, but Not in Melanoma Progression. *PLoS One, 10*(6), e0129219. doi:10.1371/journal.pone.0129219

Vandame, P., Spriet, C., Trinel, D., Gelaude, A., Caillau, K., Bompard, C., . . . Bodart, J. F. (2014). The spatio-temporal dynamics of PKA activity profile during mitosis and its

correlation to chromosome segregation. *Cell Cycle, 13*(20), 3232-3240. doi:10.4161/15384101.2014.950907

Vang, A. G., Ben-Sasson, S. Z., Dong, H., Kream, B., DeNinno, M. P., Claffey, M. M., . . . Brocke, S. (2010). PDE8 regulates rapid Teff cell adhesion and proliferation independent of ICER. *PLoS One, 5*(8), e12011. doi:10.1371/journal.pone.0012011

Vig, M., George, A., Sen, R., Durdik, J., Rath, S., & Bal, V. (2002). Commitment of activated T cells to secondary responsiveness is enhanced by signals mediated by cAMP-dependent protein kinase A-I. *Mol Pharmacol, 62*(6), 1471-1481.

Vijayaraghavan, S., Goueli, S. A., Davey, M. P., & Carr, D. W. (1997). Protein kinase A-anchoring inhibitor peptides arrest mammalian sperm motility. *J Biol Chem, 272*(8), 4747-4752.

Vo, N., Klein, M. E., Varlamova, O., Keller, D. M., Yamamoto, T., Goodman, R. H., & Impey, S. (2005). A cAMP-response element binding protein-induced microRNA regulates neuronal morphogenesis. *Proc Natl Acad Sci U S A, 102*(45), 16426-16431. doi:10.1073/pnas.0508448102

Walsh, D. A., Perkins, J. P., & Krebs, E. G. (1968). An adenosine 3',5'-monophosphate-dependant protein kinase from rabbit skeletal muscle. *J Biol Chem, 243*(13), 3763-3765.

Wayman, G. A., Tokumitsu, H., & Soderling, T. R. (1997). Inhibitory cross-talk by cAMP kinase on the calmodulin-dependent protein kinase cascade. *J Biol Chem, 272*(26), 16073-16076.

Wettenhall, R. E., & Morgan, F. J. (1984). Phosphorylation of hepatic ribosomal protein S6 on 80 and 40 S ribosomes. Primary structure of S6 in the region of the major phosphorylation sites for cAMP-dependent protein kinases. *J Biol Chem, 259*(4), 2084-2091.

Xiao, Q., Miao, B., Bi, J., Wang, Z., & Li, Y. (2016). Prioritizing functional phosphorylation sites based on multiple feature integration. *Sci Rep, 6*, 24735. doi:10.1038/srep24735

Xiong, R., Rao, P., Kim, S., Li, M., Wen, X., & Yuan, W. (2015). Herpes Simplex Virus 1 US3 Phosphorylates Cellular KIF3A To Downregulate CD1d Expression. *J Virol, 89*(13), 6646-6655. doi:10.1128/JVI.00214-15

Yao, C., Sakata, D., Esaki, Y., Li, Y., Matsuoka, T., Kuroiwa, K., . . . Narumiya, S. (2009). Prostaglandin E2-EP4 signaling promotes immune inflammation through Th1 cell differentiation and Th17 cell expansion. *Nat Med, 15*(6), 633-640. doi:10.1038/nm.1968

Yip, Y. Y., Yeap, Y. Y., Bogoyevitch, M. A., & Ng, D. C. (2014). cAMP-dependent protein kinase and c-Jun N-terminal kinase mediate stathmin phosphorylation for the maintenance of interphase microtubules during osmotic stress. *J Biol Chem, 289*(4), 2157-2169. doi:10.1074/jbc.M113.470682

Zhang, L., Zambon, A. C., Vranizan, K., Pothula, K., Conklin, B. R., & Insel, P. A. (2008). Gene expression signatures of cAMP/protein kinase A (PKA)-promoted, mitochondrial-dependent apoptosis. Comparative analysis of wild-type and cAMP-deathless S49 lymphoma cells. *J Biol Chem, 283*(7), 4304-4313. doi:10.1074/jbc.M708673200

Zhou, X. M., Liu, Y., Payne, G., Lutz, R. J., & Chittenden, T. (2000). Growth factors inactivate the cell death promoter BAD by phosphorylation of its BH3 domain on Ser155. *J Biol Chem, 275*(32), 25046-25051. doi:10.1074/jbc.M002526200

## Appendix A: Supplemental figures and tables

### Supplemental Figure 1

### Cyclic AMP measurements comparing 50 µM IBMX against 200 µM IBMX

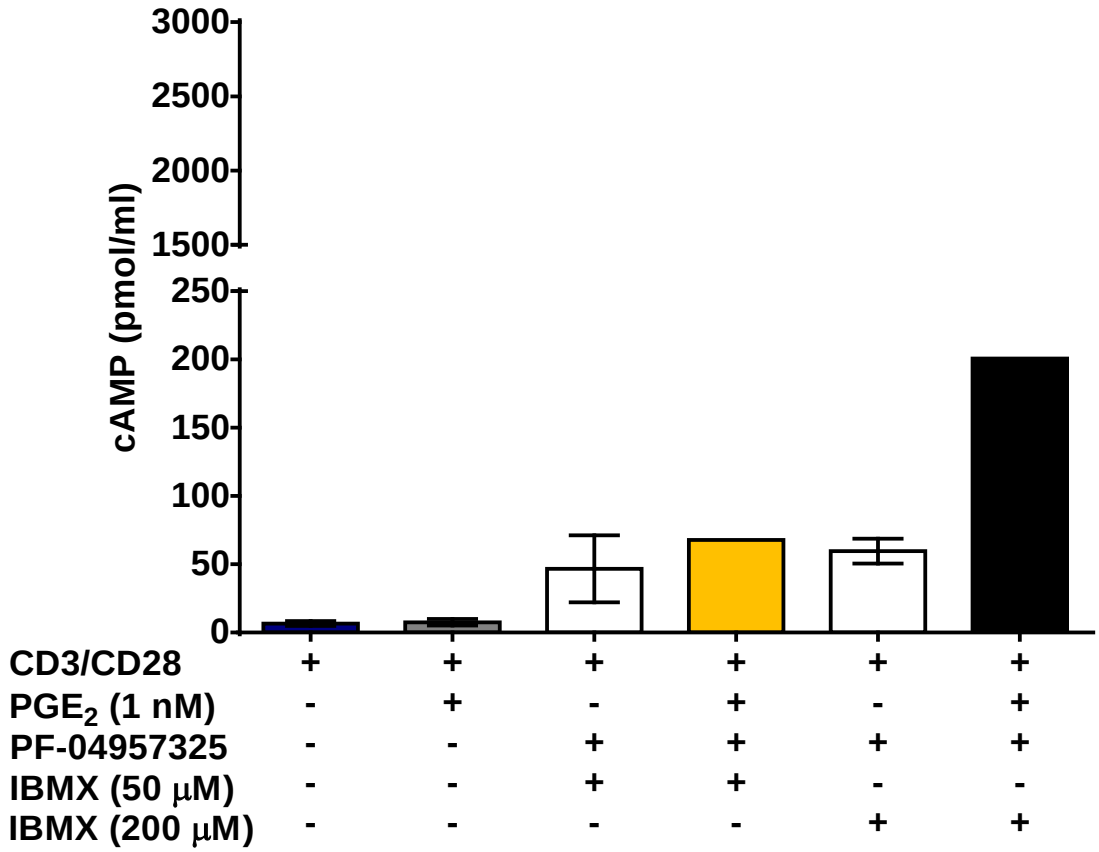


**cAMP Measurements.** 1X10^7 Jurkat cells were treated as indicated. Cells were briefly centrifuged and the supernate discarded. Cell pellets were lysed by adding 1ml of 1:99 mixture of 11.65 M HCL, and 95% EtOH. Pellets were dispersed using a P1000 pipet tip, and vortexed. Lysate was incubated at room temperature for 30 min. Following incubation, the extraction volume was transferred to a fresh microfuge tube, and dried in a speed vac. cAMP was re-suspended in 150 µl of 0.1 M HCl, acetylated, and assayed using a cAMP ELISA kit according to the manufacturer's recommendations (Cayman Biochemical)

## Supplemental Figure 2

## Outline of label-free mass spectrometry workflow and LC/MS/MS peptide identification efficiency

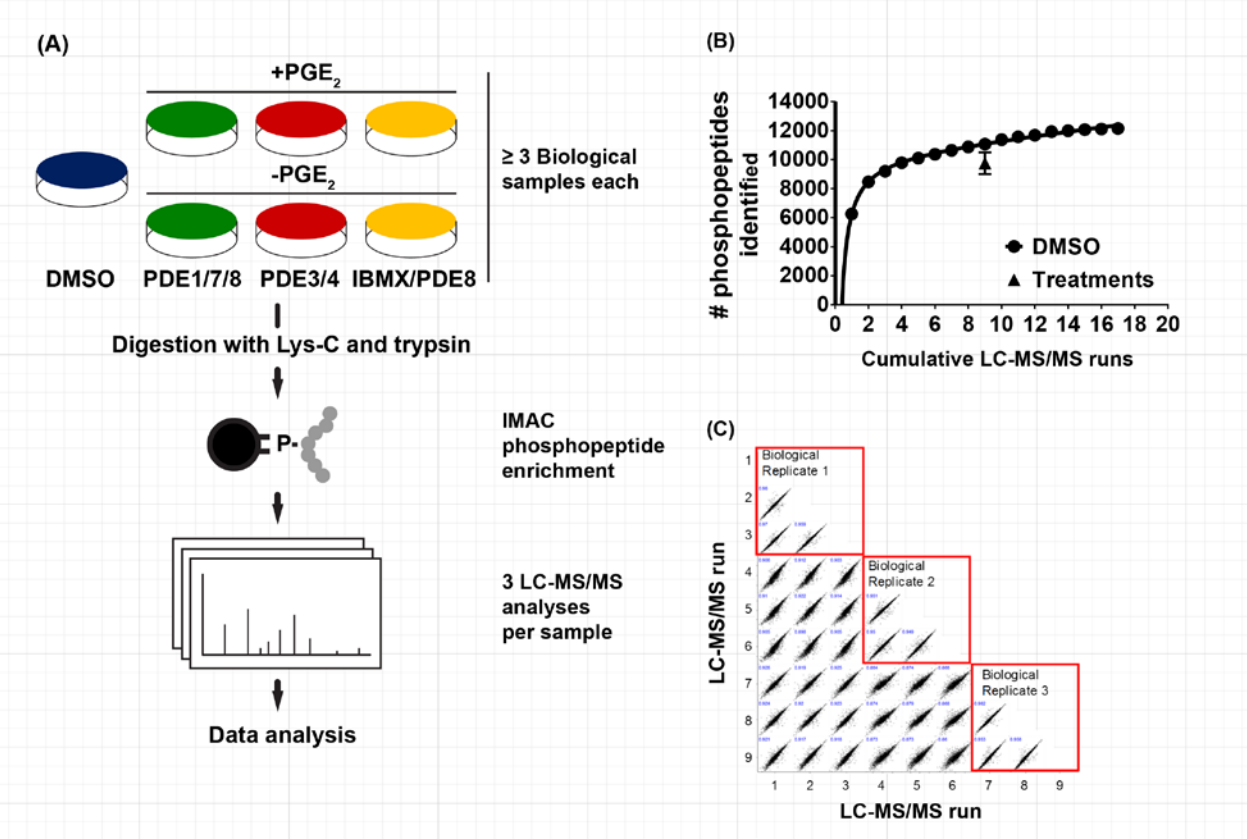


**Legend** (A) Jurkat ($5x10^6$) cells were cultured at 37°C, 5% $CO_2$ for one week in RPMI, 10% FBS, 2mM Glutamine,100 U/ml Penicillin, and 100 µg/ml Streptomycin. 24 hours prior to experiment cells were washed and serum starved for 16 hours. After 16 hours, cells were synchronized by culturing in 50% FBS for 2 hours, followed by 1 hour of culture in serum free RPMI. Cells then were concurrently treated as indicated: 0.5 µg/ml CD3, 0.5 µg/ml CD28, 1 nM $PGE_2$, 200 nM IC0078, 5 µM Cilostamide, 10 µM Rolipram, 30 µM BRL50481, 200 nM PF-04957325, 50 µM IBMX, or 200 µM IBMX. Treated cultures were incubated at 37°C, 5% $CO_2$ for 20 minutes. (B) The total number of phosphopeptides identified in DMSO and $PGE_2$ conditions, with reported intensities, were counted and plotted as a function of the cumulative number of LC-MS/MS runs ● DMSO, ■ $PGE_2$ (C). A scatter plot assessing the reproducibility

of LC-MS/MS runs. The Pearson's correlation between phosphopeptide intensities between the $PGE_2$ IBMX/PF-04957325 LC-MS/MS runs. are listed in blue. Red boxes highlight biological replicates, and analytical LC-MS/MS runs.

## Supplemental Figure 3

## Distribution of the canonical PKA sequence compared to predicted phosphorylating kinase

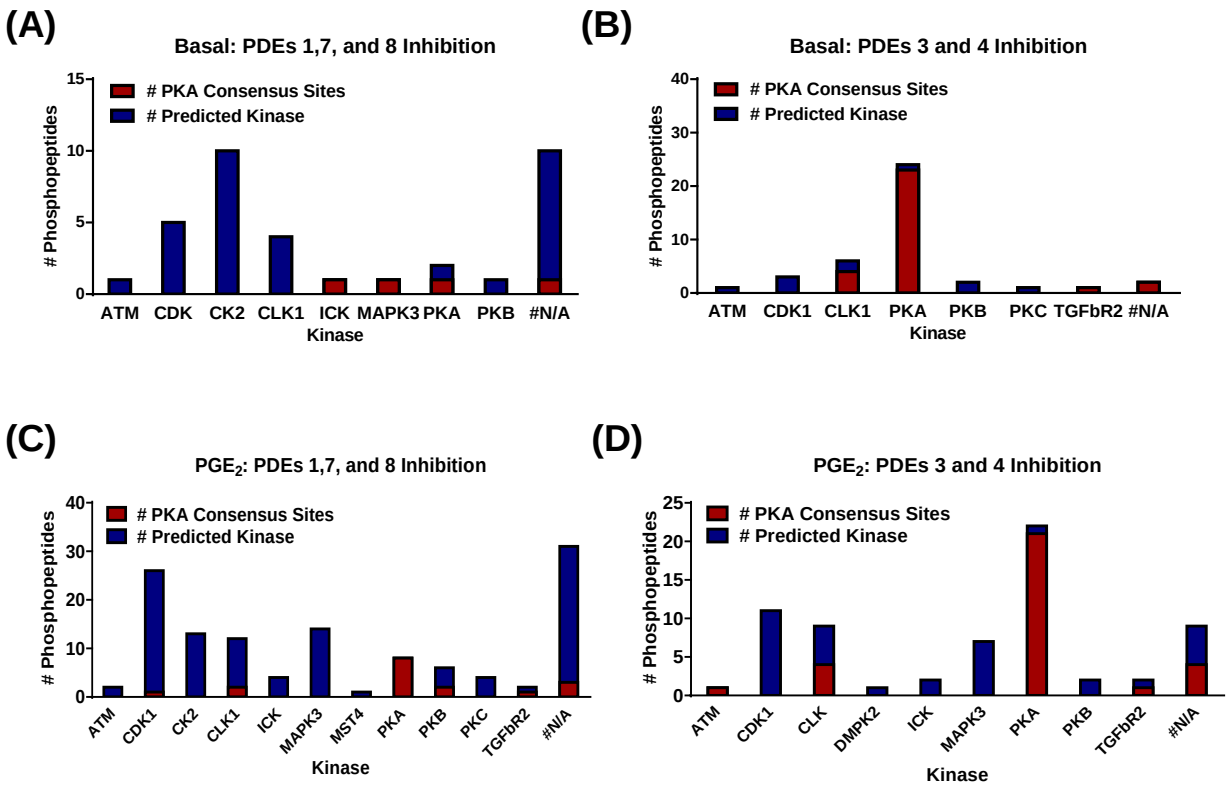


**Frequency of canonical PKA sequences that occur at sites predicted to be phosphorylated by PKA (or other kinases)**. A truncated peptide sequence of 4 amino acid residues flanking the regulated phosphosite was used as an input sequence in NetPhorest to predict kinases responsible for phosphorylating identified sites. Threshold score was set at 0.21.

## Supplemental Figure 4

## Identification of significantly regulated phosphopeptides

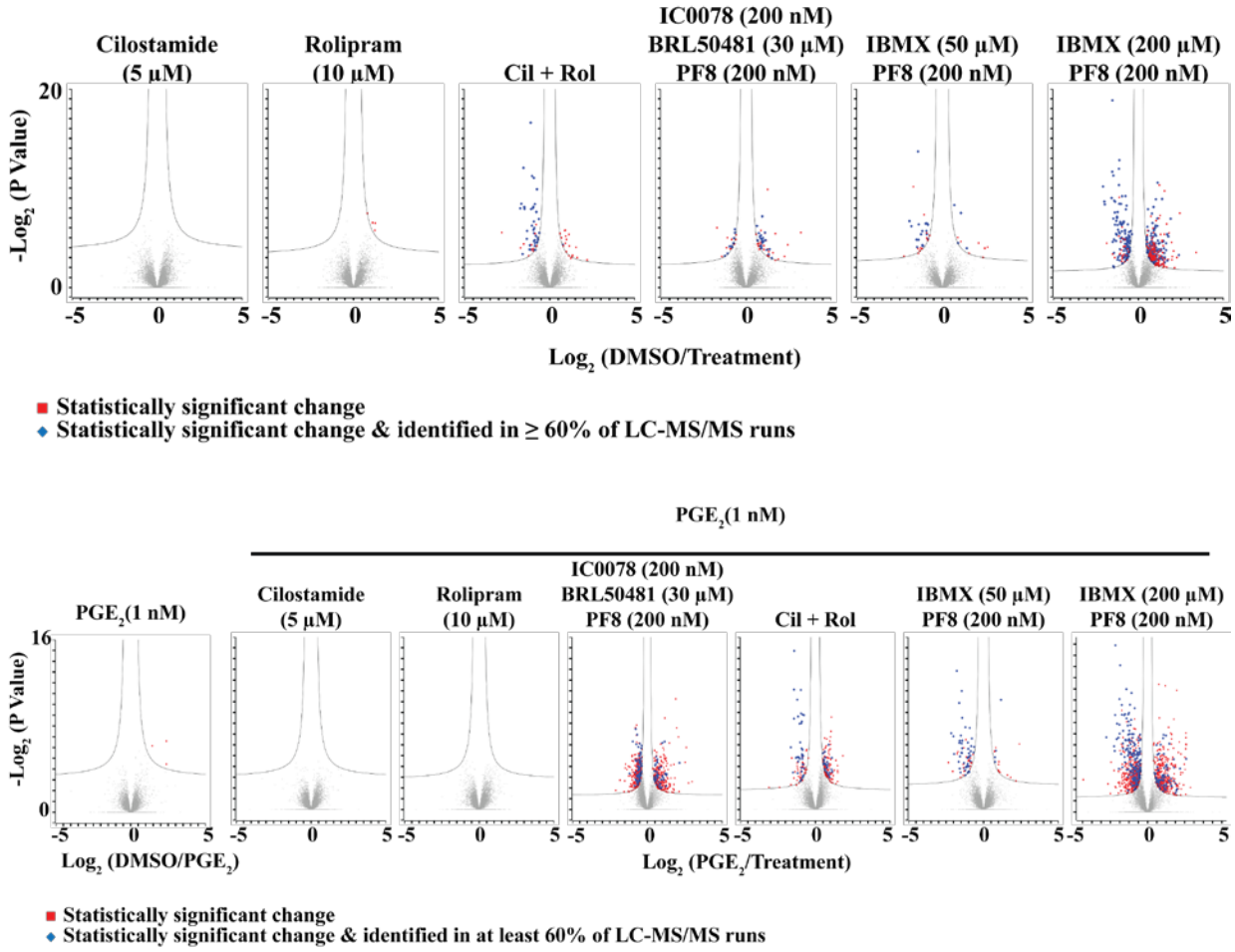


**Inhibiting multiple PDEs increase the number and magnitude of phosphorylation changes**
Volcano plots of the number of phosphosites significantly modulated compared to DMSO as a subset of the total proteome is presented as the log ratio of the DMSO intensity over the PDE inhibitor intensity plotted against the negative log of the P-value. Red squares are phosphosites significantly modulated over $PGE_2$. Blue diamonds are significantly regulated sites that occur in at least 60% of LC-MS/MS runs.

**Supplemental Figure 5.**

**STRING analysis interaction network of proteins with phosphosites regulated by 200 μM IBMX and 200 nM PDE8 inhibitor**

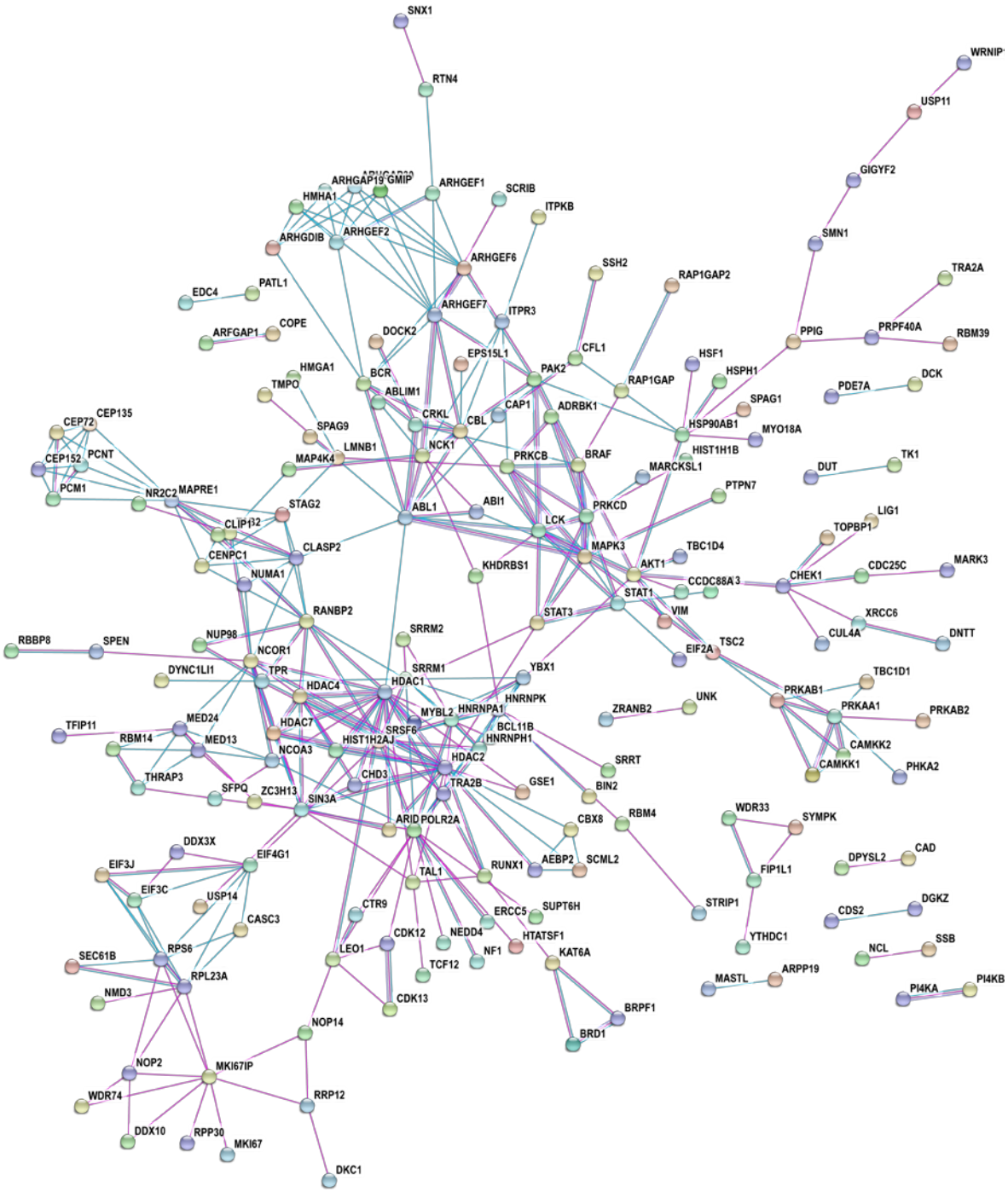

**STRING analysis to identify interacting proteins.** A gene list was generated from statistically significantly regulated phosphosites modulated by 200 uM IBMX, and PDE8 inhibition, both in the basal and $PGE_2$ stimulated condition. The list was submitted to the STRING analysis web portal to query the "Experiments" and "Databases" source options, with a minimum interaction score of 0.700. For visual clarity, disconnected nodes were omitted from the interaction map.

## Supplemental Figure 6

## GO analysis showing network of pathways and biological processes whose constituent proteins have phosphosites that are regulated by combination PDE 1, 7, and 8 inhibition.

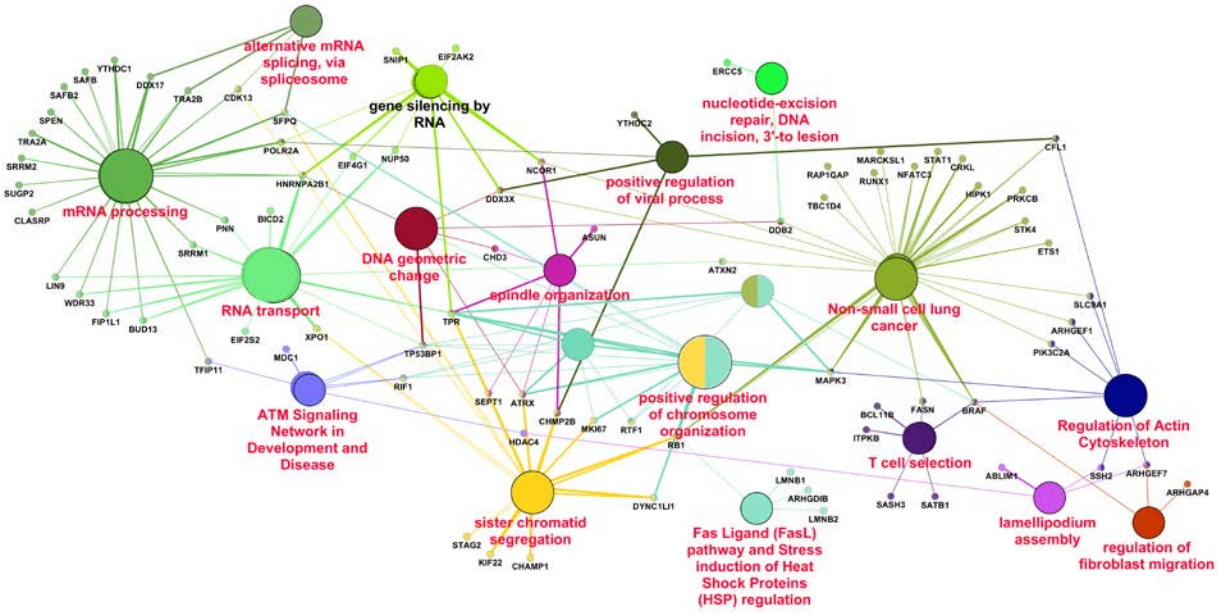


**Potential biological processes regulated by PDE1, 7, and 8 inhibition.** Gene ontology (GO) analysis was performed using the ClueGo Cytoscape plug in. A list of unique proteins, regulated by PDE 1, 7, and 8 inhibition were generated from the statistically significant regulated phosphosites. Each list was used to query the KEGG, Gene Ontology—biological function database, and Wikipathways. ClueGo parameters were set as indicated: Go Term Fusion selected; only display pathways with p values ≤ .05; GO tree interval, all levels; GO term minimum # genes, 3; threshold of 4% of genes per pathway; and kappa score of 0.42. Gene ontology terms are presented as nodes and clustered together based on the similarity of genes present in each term or pathway.

## Supplemental Table 1

## List of genes comprising GO terms in functional cluster regulated by PDE1, 7, and 8 inhibition

| Cluster | GO Term | Term P Value | Group P Value | Associated Genes Found |
|---|---|---|---|---|
| | alternative mRNA splicing, via spliceosome | 21.0E-3 | 3.0E-3 | [CDK13, DDX17, ***SFPQ***, TRA2B] |
| | nucleotide-excision repair, DNA incision, 3'-to lesion | 28.0E-3 | 3.5E-3 | [BIVM-ERCC5, DDB2, ERCC5] |
| | Fas Ligand (FasL) pathway and Stress induction of Heat Shock Proteins (HSP) regulation | 15.0E-3 | 2.1E-3 | [***ARHGDIB***, ***LMNB1***, LMNB2, ***RB1***] |
| | Regulation of Actin Cytoskeleton | 1.1E-3 | 200.0E-6 | [ARHGEF1, ***ARHGEF7***, ***BRAF***, ***CFL1***, ***MAPK3***, ***PIK3C2A***, ***SLC9A1***, SSH2] |
| | spindle organization | 8.9E-3 | 1.4E-3 | [ASUN, ATRX, ***CHD3***, ***CHMP2B***, ***NCOR1***, SEPT1, TPR] |
| | regulation of fibroblast migration | 49.0E-3 | 1.8E-3 | [ARHGAP4, ***ARHGEF7***, ***BRAF***] |
| | lamellipodium assembly | 39.0E-3 | 3.4E-3 | [ABLIM1, ***ARHGEF7***, ***HDAC4***, SSH2] |
| | DNA geometric change | 3.9E-3 | 620.0E-6 | [ATRX, ***CHD3***, DDB2, DDX3X, HNRNPA2B1, ***TP53BP1***] |
| | positive regulation of viral process | 46.0E-3 | 3.3E-3 | [***CFL1***, ***CHMP2B***, DDX3X, POLR2A, YTHDC2] |
| | ATM Signaling Network in Development and Disease | 17.0E-3 | 3.7E-3 | [***HDAC4***, MDC1, RIF1, ***TP53BP1***] |
| | double-strand break repair via nonhomologous end joining | 47.0E-3 | 3.7E-3 | [MDC1, RIF1, TFIP11, ***TP53BP1***] |
| | T cell selection | 16.0E-3 | 1.4E-3 | [***BCL11B***, ***BRAF***, FASN, ITPKB] |
| | alpha-beta T cell differentiation | 23.0E-3 | 1.4E-3 | [***BCL11B***, ***BRAF***, ITPKB, SASH3, SATB1] |
| | gene silencing by RNA | 5.1E-3 | 580.0E-6 | [EIF4G1, HNRNPA2B1, ***NCOR1***, ***NUP50***, POLR2A, SNIP1, TPR] |
| | negative regulation of translation | 8.9E-3 | 580.0E-6 | [DDX3X, ***EIF2AK2***, EIF4G1, HNRNPA2B1, ***NCOR1***, SNIP1, TPR] |
| | gene silencing by miRNA | 36.0E-3 | 580.0E-6 | [EIF4G1, HNRNPA2B1, ***NCOR1***, SNIP1] |

## Supplemental Table 1 (continued)

## List of genes comprising GO terms in functional cluster regulated by PDE1, 7, and 8 inhibition

| Cluster | GO Term | Term P Value | Group P Value | Associated Genes Found |
|---|---|---|---|---|
| | Thyroid cancer | 41.0E-3 | 62.0E-6 | [***BRAF***, ***MAPK3***, TPR] |
| | regulation of chromosome segregation | 3.2E-3 | 62.0E-6 | [ATRX, DYNC1LI1, MKI67, ***RB1***, ***SFPQ***, TPR] |
| | regulation of chromatin organization | 14.0E-3 | 62.0E-6 | [ATRX, ***MAPK3***, MKI67, RIF1, ***RTF1***, ***TP53BP1***, TPR] |
| | regulation of sister chromatid cohesion | 21.0E-3 | 62.0E-6 | [ATRX, ***RB1***, ***SFPQ***] |
| | positive regulation of chromatin organization | 31.0E-3 | 62.0E-6 | [***MAPK3***, RIF1, ***RTF1***, ***TP53BP1***, TPR] |
| | positive regulation of chromosome organization | 280.0E-6 | 62.0E-6 | [ATRX, HNRNPA2B1, ***MAPK3***, ***RB1***, RIF1, ***RTF1***, ***SFPQ***, ***TP53BP1***, TPR] |
| | mRNA Processing | 3.8E-3 | 11.0E-9 | [***CLASRP***, HNRNPA2B1, POLR2A, ***SFPQ***, SRRM1, SUGP2, TRA2B] |
| | mRNA processing | 6.7E-9 | 11.0E-9 | [BUD13, CDK13, ***CLASRP***, DDX17, FIP1L1, HNRNPA2B1, LIN9, PNN, POLR2A, SAFB, SAFB2, ***SFPQ***, SPEN, SRRM1, SRRM2, SUGP2, TFIP11, TRA2A, TRA2B, ***WDR33***, YTHDC1] |
| | RNA splicing | 34.0E-9 | 11.0E-9 | [BUD13, CDK13, ***CLASRP***, DDX17, FIP1L1, HNRNPA2B1, LIN9, PNN, POLR2A, ***SFPQ***, SPEN, SRRM1, SRRM2, SUGP2, TFIP11, TRA2A, TRA2B, ***WDR33***, YTHDC1] |
| | regulation of RNA splicing | 45.0E-3 | 11.0E-9 | [DDX17, HNRNPA2B1, POLR2A, TRA2B, YTHDC1] |
| | regulation of mRNA processing | 7.3E-3 | 11.0E-9 | [DDX17, HNRNPA2B1, SAFB, SAFB2, TRA2B, YTHDC1] |
| | mRNA splicing, via spliceosome | 20.0E-9 | 11.0E-9 | [BUD13, CDK13, DDX17, FIP1L1, HNRNPA2B1, LIN9, PNN, POLR2A, ***SFPQ***, SPEN, SRRM1, SRRM2, TFIP11, TRA2A, TRA2B, ***WDR33***, YTHDC1] |

## Supplemental Table 1 (continued)

## List of genes comprising GO terms in functional cluster regulated by PDE1, 7, and 8 inhibition

| Cluster | GO Term | Term P Value | Group P Value | Associated Genes Found |
|---|---|---|---|---|
| | RNA transport | 14.0E-3 | 2.4E-6 | [***EIF2S2***, EIF4G1, ***NUP50***, PNN, SRRM1, TPR, ***XPO1***] |
| | ribonucleoprotein complex localization | 46.0E-6 | 2.4E-6 | [BUD13, FIP1L1, HNRNPA2B1, LIN9, ***NUP50***, SRRM1, TPR, ***WDR33***, ***XPO1***] |
| | RNA transport | 25.0E-6 | 2.4E-6 | [ATXN2, BICD2, BUD13, FIP1L1, HNRNPA2B1, LIN9, ***NUP50***, SRRM1, TPR, ***WDR33***, ***XPO1***] |
| | intracellular transport of virus | 16.0E-3 | 2.4E-6 | [***NUP50***, TPR, ***XPO1***] |
| | mRNA transport | 210.0E-6 | 2.4E-6 | [BICD2, BUD13, FIP1L1, HNRNPA2B1, ***NUP50***, SRRM1, TPR, ***WDR33***, ***XPO1***] |
| | protein export from nucleus | 690.0E-6 | 2.4E-6 | [BUD13, FIP1L1, HNRNPA2B1, ***NUP50***, SRRM1, ***TP53BP1***, TPR, ***WDR33***, ***XPO1***] |
| | regulation of chromosome segregation | 3.2E-3 | 120.0E-9 | [ATRX, DYNC1LI1, MKI67, ***RB1***, ***SFPQ***, TPR] |
| | sister chromatid segregation | 640.0E-6 | 120.0E-9 | [ATRX, CHAMP1, ***CHMP2B***, DYNC1LI1, KIF22, ***RB1***, ***SFPQ***, STAG2, TPR, ***XPO1***] |
| | metaphase plate congression | 27.0E-3 | 120.0E-9 | [CHAMP1, ***CHMP2B***, KIF22, SEPT1] |
| | sister chromatid cohesion | 19.0E-3 | 120.0E-9 | [ATRX, KIF22, ***RB1***, ***SFPQ***, STAG2, ***XPO1***] |
| | mitotic sister chromatid segregation | 6.0E-3 | 120.0E-9 | [ATRX, CHAMP1, ***CHMP2B***, DYNC1LI1, KIF22, ***RB1***, TPR] |
| | regulation of mitotic nuclear division | 9.5E-3 | 120.0E-9 | [ATRX, CDK13, ***CHMP2B***, DYNC1LI1, MKI67, ***RB1***, TPR] |
| | regulation of sister chromatid cohesion | 21.0E-3 | 120.0E-9 | [ATRX, ***RB1***, ***SFPQ***] |
| | positive regulation of chromosome organization | 280.0E-6 | 120.0E-9 | [ATRX, HNRNPA2B1, ***MAPK3***, ***RB1***, RIF1, ***RTF1***, ***SFPQ***, ***TP53BP1***, TPR] |

## Supplemental Table 1 (continued)

## List of genes comprising GO terms in functional cluster regulated by PDE1, 7, and 8 inhibition

| Cluster | GO Term | Term P Value | Group P Value | Associated Genes Found |
|---|---|---|---|---|
| | Dorso-ventral axis formation | 39.0E-3 | 860.0E-12 | [***BRAF***, ***ETS1***, ***MAPK3***] |
| | B cell receptor signaling pathway | 16.0E-3 | 860.0E-12 | [***MAPK3***, ***NFATC3***, ***PRKCB***] |
| | Fc gamma R-mediated phagocytosis | 26.0E-3 | 860.0E-12 | [***CFL1***, CRKL, ***MAPK3***, ***MARCKSL1***, ***PRKCB***] |
| | Long-term potentiation | 40.0E-3 | 860.0E-12 | [***BRAF***, ***MAPK3***, ***PRKCB***] |
| | Thyroid hormone signaling pathway | 12.0E-3 | 860.0E-12 | [***MAPK3***, ***NCOR1***, ***PRKCB***, ***SLC9A1***, ***STAT1***, ***TBC1D4***] |
| | Hepatitis B | 6.4E-3 | 860.0E-12 | [DDB2, DDX3X, ***MAPK3***, ***NFATC3***, ***PRKCB***, ***RB1***, ***STAT1***] |
| | Renal cell carcinoma | 46.0E-3 | 860.0E-12 | [***BRAF***, CRKL, ***ETS1***, ***MAPK3***] |
| | Pancreatic cancer | 45.0E-3 | 860.0E-12 | [***BRAF***, ***MAPK3***, ***RB1***, ***STAT1***] |
| | Glioma | 45.0E-3 | 860.0E-12 | [***BRAF***, ***MAPK3***, ***PRKCB***, ***RB1***] |
| | Thyroid cancer | 41.0E-3 | 860.0E-12 | [***BRAF***, ***MAPK3***, TPR] |
| | Melanoma | 31.0E-3 | 860.0E-12 | [***BRAF***, ***MAPK3***, ***RB1***] |
| | Chronic myeloid leukemia | 11.0E-3 | 860.0E-12 | [***BRAF***, CRKL, ***MAPK3***, ***RB1***, ***RUNX1***] |
| | Non-small cell lung cancer | 3.7E-3 | 860.0E-12 | [***BRAF***, ***MAPK3***, ***PRKCB***, ***RB1***, ***STK4***] |
| | Human Thyroid Stimulating Hormone (TSH) signaling pathway | 8.6E-3 | 860.0E-12 | [***BRAF***, ***MAPK3***, RAP1GAP, ***RB1***, ***STAT1***] |
| | Signaling Pathways in Glioblastoma | 17.0E-3 | 860.0E-12 | [***BRAF***, ***MAPK3***, ***PIK3C2A***, ***PRKCB***, ***RB1***] |
| | B Cell Receptor Signaling Pathway | 30.0E-3 | 860.0E-12 | [***BRAF***, CRKL, ***ETS1***, ***NFATC3***, ***PRKCB***] |
| | Kit receptor signaling pathway | 36.0E-3 | 860.0E-12 | [CRKL, ***MAPK3***, ***PRKCB***, ***STAT1***] |
| | EGF/EGFR Signaling Pathway | 11.0E-3 | 860.0E-12 | [ARHGEF1, ATXN2, ***BRAF***, ***CFL1***, CRKL, ***PRKCB***, ***STAT1***] |
| | epithelial cell apoptotic process | 31.0E-3 | 860.0E-12 | [***BRAF***, FASN, HIPK1, ***RB1***, ***STK4***] |
| | positive regulation of chromatin organization | 31.0E-3 | 860.0E-12 | [***MAPK3***, RIF1, ***RTF1***, ***TP53BP1***, TPR] |
| | hepatocyte apoptotic process | 11.0E-3 | 860.0E-12 | [FASN, ***RB1***, ***STK4***] |

**Supplemental Table 1 (continued). List of genes comprising GO terms in functional cluster regulated by PDE1, 7, and 8 inhibition.** Gene ontology (GO) analysis was performed using the ClueGo Cytoscape plug in. Lists of unique proteins for PDEs 1, 7, and 8 inhibitor treatment were generated from the statistically significant regulated phosphosites. Each list was used to query KEGG, Gene Ontology—biological function database, and Wikipathways. ClueGo parameters were set as indicated: Go Term Fusion selected; only display pathways with p values ≤0 .05; GO tree interval, all levels; GO term minimum # genes, 3; threshold of 4% of genes per pathway; and kappa score of 0.42. **Bolded genes** have regulated phosphosites predicted to be functional. In addition, **Red bolded genes** are sites with a PKA consensus site.

## Supplemental Table 2

## List of genes comprising GO terms in functional cluster regulated by PDE3, and 4 inhibition

| Cluster | GO Term | Term P Value | Group P Value | Associated Genes Found |
|---|---|---|---|---|
| | double-strand break repair via nonhomologous end joining | 5.3E-3 | 2.6E-3 | **[MDC1, *RIF1*, SMC5]** |
| | Pathways Affected in Adenoid Cystic Carcinoma | 7.3E-3 | 4.9E-3 | [ARID1A, HIST1H1E, ***MAP2K2***] |
| | establishment of spindle orientation | 1.1E-3 | 490.0E-6 | [ARHGEF2, MAP4, ***NUMA1***] |
| | Chronic myeloid leukemia | 3.2E-3 | 2.8E-3 | [***ABL1***, ***BAD***, ***MAP2K2***] |
| | Amyotrophic lateral sclerosis (ALS) | 2.9E-3 | 2.8E-3 | [ALS2, ***BAD***, ***MAP2K2***] |
| | histone H3-K27 trimethylation | 98.0E-6 | 53.0E-6 | [HIST1H1C, HIST1H1D, HIST1H1E] |
| | peptidyl-lysine trimethylation | 200.0E-6 | 53.0E-6 | [HIST1H1C, HIST1H1D, HIST1H1E, PWP1] |
| | histone lysine methylation | 100.0E-6 | 53.0E-6 | [HIST1H1C, HIST1H1D, HIST1H1E, PWP1, ***RIF1***, SNW1] |
| | histone H3-K4 methylation | 730.0E-6 | 53.0E-6 | [HIST1H1C, HIST1H1D, HIST1H1E, SNW1] |
| | Regulation of Microtubule Cytoskeleton | 4.1E-3 | 270.0E-6 | [***ABL1***, CLIP1, ***STMN1***] |
| | regulation of microtubule cytoskeleton organization | 200.0E-6 | 270.0E-6 | [***ABL1***, ARHGEF2, CLIP1, GAS2L1, RANBP2, ***STMN1***] |
| | negative regulation of microtubule polymerization or depolymerization | 1.6E-3 | 270.0E-6 | [ARHGEF2, GAS2L1, ***STMN1***] |
| | regulation of microtubule polymerization | 1.7E-3 | 270.0E-6 | [***ABL1***, CLIP1, ***STMN1***] |
| | protein depolymerization | 3.5E-3 | 270.0E-6 | [ARHGEF2, GAS2L1, MICAL1, ***STMN1***] |

**Legend -- List of genes comprising GO terms in functional cluster regulated by PDE3, and 4 inhibition.** Gene ontology (GO) analysis was performed using the ClueGo Cytoscape plug in. Lists of unique proteins for PDEs 3 and 4inhibitor treatment were generated from the statistically significant regulated phosphosites. Each list was used to query KEGG, Gene Ontology—biological function database, and Wikipathways. ClueGo parameters were set as indicated: Go Term Fusion selected; only display pathways with p values ≤ 0.05; GO tree interval, all levels; GO term minimum # genes, 3; threshold of 4% of genes per pathway; and kappa score of 0.42. **Bolded genes** have regulated phosphosites predicted to be functional. In addition, **Red bolded genes** are sites with a PKA consensus sequence.

# Vita

Michael Claude G. Beltejar

**Education**:

Molecular Cellular Biology Program Ph.D. 2009-2017
University of Washington
Seattle, WA

B.S. in Biology with a minor in Biochemistry (Summa Cum Laude) May 2000
College of Notre Dame (Notre Dame de Namur University)
Belmont, CA

**Teaching Experience:**

**University of Washington Seattle, WA Jan 2011-Mar 2011**
**Teaching Assistant, Biology Department**
Lead quiz sections in which undergraduate students were instructed on how to read and interpret scientific articles.

**College of Notre Dame Belmont, CA Aug 1998- Dec 1998**
**Lab Assistant, Biology Department**

Aided professor in the instruction of general biology lab. Instructed student in general laboratory practices and common calculations. Aided students in laboratory notebook record and design.

**Research Experience**:

**University of Washington Seattle, WA Jun 2010- Mar 2017**
**Beavo Lab (Thesis Lab)**

Used mass spectrometry based proteomics to characterize cAMP functional domains created by PDE inhibition.

**University of Washington Seattle, WA Mar 2010- Jun 2010**
**Vasioukhin Lab (Rotation Student)**

**Fred Hutch Cancer Research Center**

Rotation project objective: verify the binding interactions between human Lgl and previously identified putative binding partners *in vivo.* Question posed: Can interacting partners suggest functions and mechanisms of the human Lgl protein?

**University of Washington Seattle, WA Jan 2010- Mar 2010**
**Beavo Lab (Rotation Student)**
Rotation project objectives: 1) identify PDE inhibitors that specifically modulated FXIII, MMP-7 and IL-10 2) determine if GM-CSF or M-CSF (macrophage colony stimulating factor) derived macrophages differentially express CXCL5 in response to elevated cAMP levels. Question posed: can selective PDE inhibition could modulate the wound healing phenotype of monocyte derived macrophage cultures?

**University of Washington Seattle, WA Oct 2009- Dec 2009**
**Warren Lab (Rotation Student)**
**Fred Hutch Cancer Research Center**

Rotation project objectives: utilize spectratyping to characterize the TCR diversity from tumor infiltrating lymphocytes isolated from patient renal cell carcinoma primary tissue and PBMCs recovered at the time of surgery. The questions posed were: 1) is there an oligoclonal expansion of T cell populations indicative of an immune antitumor response? 2) can an observed oligoclonal lymphocytic expansion observed in the tumor be identified in peripheral circulation

**Macrogenics So San Francisco, CA Jul 2008- Aug 2009**

Cloned target proteins into mammalian expression vectors. Performed RNAi knockdown studies of target proteins to help establish definitive antibody binding to target proteins. Performed and optimized soft agar assays using ATCC cell lines to screen for antibody mediated cell death

**Raven Biotechnologies So San Francisco, CA May 2003-Jul 2008**
**Research Associate**

Cloned antibody variable genes into mammalian expression vectors. Prepared mammalian expression vectors for stable and transient transfection. Developed antibody production cell lines for two product candidates. Performed and optimized quantitative PCR based assays to measure tumor mass (for in vivo studies), quantify contaminant CHO DNA in antibody preparations, and to identify Fc gamma receptor IIIa polymorphisms in clinical patient samples. Evaluated antibody mediated CDC (complement dependent cytotoxicity), and ADCC (antibody-dependent cell-mediated cytotoxicity) for selected product candidates. Performed CDC and ADCC on cell lines treated with chemotherapeutics or radiation to evaluate conditioning mediated antibody effects. Established primary cultures from fetal pancreatic tissue for use in beta cell

differentiation studies. Validated quantitative PCR primers for housekeeping genes and beta cell markers for beta cell differentiation analysis.

**Eos Biotechnology So San Francisco, CA Nov 2000-Apr 2003**
**Associate Scientist**
**Antibody Engineering**

Expressed in E. *coli*: ScFv, ScFv-Fc fusions, Fab and Fab' antibody fragments. Aided in the expression optimization of antibody fragments in E. *coli* Purified antibody fragments from E. *coli* periplasm or culture media, using IMAC and/or 85mmune-affinity chromatography. Characterized antibody fragments for purity, specificity, and affinity (SDS-PAGE, ELISA, Western Blot, and Mass Spectrometry). Evaluated several endotoxin removal protocols, and optimized final protocol for application on Fab antibody fragments. Used phage display to select for ScFv against Eos target proteins. Cloned antibody variable genes into E. *coli* expression vectors.

**Veterans Affairs Medical Center**
**Stanford, CA**
**Aug 1999-May 2000**
**Research Assistant**

Performed DNA gel electrophoresis, protein assays, and tissue culture. Performed DNA extraction, and purification. Aided in the extraction and isolation of mouse bone marrow, for tissue culture and the evaluation of bone differentiating factors. Performed cell-staining assays. Aided in the evaluation of colony counting software.

**Publications**:
Loo D, Beltejar C, Hooley J, Xu X. Primary and multi-passage culture of human fetal kidney epithelial progenitor cells. Methods Cell Biol. 2008;86:241-55.

**Awards:**
Cell and Molecular Biology training grant recipient (2011-2013)